

ARISTOTLE UNIVERSITY OF THESSALONIKI
SCHOOL OF GEOLOGY
DEPARTMENT OF GEOLOGY

KARAGIANNIS TSANIDIS DIMITRIOS CHRISTOS
GEOLOGIST

A Computational Model for Optimum Wellbore Completion Design Using PipeSim

Presented to the Inter-Institutional Postgraduate Studies Program

“Hydrocarbon Exploration and Exploitation”

in Partial Fulfilment of the Requirements for the Degree of

Master in Science

Thessaloniki 2023



The Thesis Committee for *Karagiannis Tsanidis Dimitrios Christos* Certifies That This is The Approved Version of The Following Thesis:

A Computational Model for Optimum Wellbore Completion Design Using PipeSim

APPROVED BY
SUPERVISING COMMITTEE

Supervisor &

Examining committee:

Dr. Ernestos Sarris
(Assistant Professor, Advisor)

.....
Dr. Vassilis Gaganis
(Associate Professor, Member)

.....
Dr. Antreas Georgakopoulos
(Professor, Member)



© Karagiannis Tsanidis Dimitrios Christos, Geologist, 2023
All rights reserved.

A Computational Model for Optimum Wellbore Completion Design Using PipeSim– *Master*
Thesis

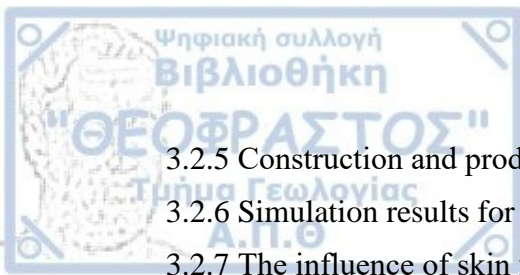
It is forbidden to copy, store, reproduce and distribute this work, in whole or in part, for commercial purposes. Reproduction, storage, and distribution are permitted for non-profit, educational or research purposes, provided the source of origin is indicated. Questions concerning the use of work for profit-making purposes should be addressed to the author.

The views and conclusions contained in this document express the author and should not be interpreted as expressing the official positions of the Aristotle University of Thessaloniki.



TABLE OF CONTENTS

TABLE OF CONTENTS.....	iii
LIST OF FIGURES	v
LIST OF TABLES.....	vii
Abstract.....	viii
Περίληψη	ix
Acknowledgement	x
CHAPTER 1 Introduction.....	1
1.1 Scope of study	1
1.2 Objectives and methods	1
1.3 Thesis summary.....	3
CHAPTER 2 Theoretical Background.....	4
2.1 Geology of the Area	4
2.1.1 Geology of the North Sea	4
2.1.2 Geology in the proximal area of the wells under study	5
2.2 Reservoir Rock and Fluid Model	9
2.3 Wellbores Description.....	12
2.3.1 Reference well 6507/7-16 S	12
2.3.2 Second reference well 31/3-3	13
2.4 The Completion String Facilities	14
2.4.1 Landing nipples	16
2.4.2 Packers.....	17
2.4.3 Sliding sleeves (SSD)	18
2.4.4 Subsurface Safety Valve (SSSV)	19
2.4.5 Wellhead assembly	19
2.5 Nodal Analysis	20
2.5.1 Well performance	22
CHAPTER 3 Numerical Simulations	24
3.1 PipeSim Software.....	24
3.2 Models Setup.....	24
3.2.1 Description of modeling procedure	24
3.2.2 Simulation results for the reference well “6507/7-16S”.....	33
3.2.3 The influence of water-cut on production	40
3.2.4 The influence of skin factor of well “6507/7-16S”	42



3.2.5 Construction and production simulation of well “well 31/3-3”	45
3.2.6 Simulation results for the well “31/3-3”	48
3.2.7 The influence of skin factor of well “31/3-3”	51
3.3 Comparison of results.....	53
3.3.1 Comment on the outflow performance	53
3.3.2 Comment on inflow performance	54
CHAPTER 4 Conclusions.....	56
4.1 Synthesis.....	56
4.2 Findings.....	56
4.3 Suggestions for improvement.....	57
References.....	59
Internet resources.....	60

LIST OF FIGURES

Figure 2.1: Location of the reference well (https://factpages.npd.no/).....	13
Figure 2.2: Wellbore position of “well 31/3-3” (Eiken and Tøndel, 2005).....	14
Figure 2.3 Well construction and completion design flow chart (Watt, 2014).....	15
Figure 2.4: Basic well completion string equipment (Watt, 2014).....	16
Figure 2.5 Landing nipple (ruifengpetrotech-en.com).....	17
Figure 2.6 Elastomer Packer (Bellarby, 2009).....	18
Figure 2.7 Slide side door (SSD). (a) Open, (b) closed (Bellarby, 2009).....	19
Figure 2.8 Sub Surface Safety Valve (SSSV) (superiorenergy.com).....	19
Figure 2.9 (a) Wellhead section and (b) X-mass tree (a: Bellarby 2009; b: camtop-oilfieldtools.com).....	20
Figure 2.10 Typical inflow, outflow performance relationships with operating point for a gas reservoir (Vo et al., 2020).....	23
Figure 3.1: Pipesim workspace interface.....	25
Figure 3.2: General input data.....	25
Figure 3.3: Well construction (geometry) and material data for the case of barefoot.....	27
Figure 3.4: Well construction (geometry) and material data for the case of cemented and perforated.....	27
Figure 3.5: Deviation survey.....	28
Figure 3.6: Downhole equipment data.....	29
Figure 3.7: Artificial lift tab (no artificial lift was simulated).....	30
Figure 3.8: Heat transfer properties considered in the simulations.....	30
Figure 3.9: Completion tab properties (reservoir, fluid model and perforations).....	31
Figure 3.10: Final well completion model for “6507/7-16S”.....	32
Figure 3.11: Nodal analysis properties.....	33
Figure 3.12 Production for tube size 2.375 and all tube embedment lengths.....	34
Figure 3.13 Production for tube size 2.875 and all tube embedment lengths.....	35
Figure 3.14 Production for tube size 3.5 and all tube embedment lengths.....	35
Figure 3.15 Production for tube size 4.5 and all tube embedment lengths.....	36
Figure 3.16 Inflow and outflow performance for all tube sizes considered.....	37
Figure 3.17 Comparison between open and closed hole.....	38
Figure 3.18: Oil production rate as a function of reservoir pressure for different values of water-cut {0:35:5}.....	40
Figure 3.19: Gas production after inserting watercut.....	41
Figure 3.20: Oil production with different skin factors for 0% water-cut.....	43
Figure 3.21: Gas production with different skin factors for 0% water-cut.....	43
Figure 3.22: Oil production with different skin factors for 35% water-cut.....	44
Figure 3.23: Gas production with different skin factors for 35% water-cut.....	44
Figure 3.24: General data of the “well 31/3-3”.....	45
Figure 3.25: Well construction (geometry) and material data for the "well 31/3-3".....	45
Figure 3.26: Downhole equipment used for the simulation of well “31/3-3”.....	46
Figure 3.27: Final well completion model for well “31/3-3”.....	47
Figure 3.28: Oil production for different reservoir pressure for the well "31/3-3".....	49
Figure 3.29: Oil production comparison between the two wells.....	49
Figure 3.30 Inflow and outflow performance for all reservoir boundary pressure conditions.....	50

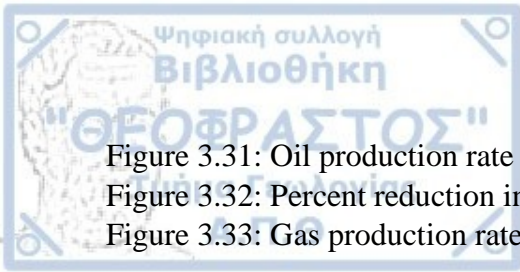


Figure 3.31: Oil production rate after inserting skin factor	51
Figure 3.32: Percent reduction in oil production due to skin.....	52
Figure 3.33: Gas production rate after inserting skin factor	52



LIST OF TABLES

Table 1.1: Simulation assumptions	2
Table 2.1: Fangst reservoir rock properties (Theuerkorn, 2012)	9
Table 3.1: Penetration depth with various tubing sizes (Halliburton.com).....	28
Table 3.2: Production with different bean size and installation depth	39
Table 3.3 Rock and Fluid properties definitions for well "31/3-3"	48



Abstract

In this work, we propose a computational model for simulating the optimum design of a wellbore with the use of PipeSim software. The input data for the simulations were obtained from an actual well at the North Sea in Norway labelled as “*well 6507/7-16 S*” but also from “*well 31/3-3*” located in the same area. Although, these wells are plugged and abandoned (P&A), their characteristics are still being used to date for calibrating models either with commercial software or for construction of proprietary codes with programming languages. The simulation is based in the widely accepted method of nodal analysis for constructing the inflow and outflow performance, accounting for the geological and thermodynamic conditions of the reservoir formation. From the analysis performed, we show that the computational model proved to be a fast and accurate tool for optimizing the well completion strategy. Also, by constructing computationally the inflow and outflow performance relationship could serve as a decision-making tool for industrial operators using cost efficient equipment.



Περίληψη

Σε αυτήν την εργασία, προτείνουμε ένα υπολογιστικό μοντέλο για προσομοίωση του βέλτιστου σχεδιασμού και ολοκλήρωσης μιας γεώτρησης με την βοήθεια του λογισμικού PipeSim. Τα δεδομένα για τις προσομοιώσεις είναι από μια πραγματική γεώτρηση που βρίσκεται στην Βόρεια Θάλασσα στην Νορβηγία επονομαζόμενη “6507/7-16S” αλλά και επίσης από την γεώτρηση “31/3-3” που βρίσκεται στην ίδια περιοχή. Αν και αυτές οι γεωτρήσεις έχουν χαρακτηριστεί ως άγονες (plug & abandoned), τα χαρακτηριστικά τους χρησιμοποιούνται μέχρι σήμερα για βαθμονόμηση μοντέλων είτε με εμπορικά λογισμικά είτε με εξειδικευμένους προγραμματιστικούς κώδικες. Η προσομοίωση είναι βασισμένη στην γνωστή αριθμητική μέθοδο των κόμβων η οποία επιλύει με ακρίβεια και ταχύτητα προβλήματα ροής από τον ταμειυτήρα στο πηγάδι και από το πηγάδι στην επιφάνεια λαμβάνοντας υπόψη τόσο τις γεωλογικές όσο και θερμοδυναμικές συνθήκες του ταμειυτήρα. Από την ανάλυση που πραγματοποιήθηκε, φαίνεται ότι το υπολογιστικό μοντέλο μπορεί να χρησιμοποιηθεί ως ένα γρήγορο και ακριβές εργαλείο για την βελτιστοποίηση ολοκλήρωσης μιας γεώτρησης. Επίσης, ο υπολογιστικός/συνθετικός προσδιορισμός της απόδοσης ροής της γεώτρησης, θα μπορούσε να χρησιμοποιηθεί ως εργαλείο λήψης αποφάσεων στη βιομηχανία μέσω βελτιστοποίησης και εξοικονομώντας προϋπολογισμό από εξοπλισμούς.

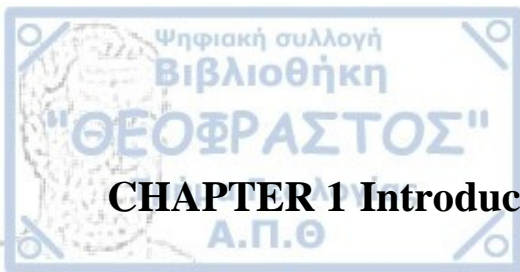


Acknowledgements

I would like to deeply thank all the Professors involved in this study. First of all, my supervisor, Assistant Professor Dr. Ernestos Sarris for his guidance and support throughout the whole process. He has always been by my side and solved many technical and theoretical problems that I had to deal with during the completion of this work. Additionally, the Head of the MSc programme *Hydrocarbons Exploration and Exploitation* Professor Andreas Georgakopoulos for his advice through the duration of my studies.

A warm thanks to my friends and fellow Master students, Mrs Ioanna Charisopoulou and Mr Nikolaos Theologis for their emotional support throughout the master's programme duration, but also for their feedback and cooperation.

Last but not least, I would like to thank my family, my mother Elpida and my father Nikos, for their financial support all these years and helping me overcome difficulties while writing this MSc thesis. I could not neglect, my brother Giannis, for his emotional support and patience given to me knowing that I had to deal with something difficult. I know they will be there my whole life.



CHAPTER 1 Introduction

1.1 Scope of study

The scope of this work is the construction of a computational model for simulating the optimum design of a wellbore with the use of PipeSim software. The analysis is based on two actual test cases in the North Sea in Norway. The two wells are named “*well 6507/7-16 S*” and “*well 31/3-3*” located in the same area. Although the data used for the simulations are from actual wells, the pumping scenarios used are entirely theoretical, and this explained by the fact that hydrocarbon companies do not make easily available wellbore data. The computational model makes use of the nodal analysis method to construct the inflow and outflow performance of each of the aforementioned wells, also accounting for the geological and thermodynamic conditions of the reservoir formation.

The purpose of this computational model is its ability to serve as a fast and accurate tool for optimizing the well completion strategy. Furthermore, by “*synthetic*” construction of the inflow and outflow performance relationship, which is heavily based on the pumping scenarios assumed for the simulations, could serve as a decision-making tool for industrial operators by managing their available funds for the well completion while balancing safe production over the life of the well. Hydrocarbon exploration and appraisal is usually quite expensive, thus correct modelling is a key element for ensuring optimum results with the least risk and the least possible cost.

1.2 Objectives and methods

The main objective of this work is the construction of a computational model that will provide the capability to investigate possible completion designs of two wells, namely, the “*well 6507/7-16 S*” and “*well 31/3-3*” and then compare the produced results from the simulations. The results for the production from the two wells are compared with the aim to determine the optimum location of the equipment (e.g., packers or Slide side doors (SSD’s)) based on the geological and thermodynamic data available from the literature. Then a sensitivity analysis is performed for the following degrees of freedom (d.o.f): (i) penetration depth and (ii) tube hydraulics (diameter). The reason for the selection of these two d.o.f’s is the fact that the penetration depth affect the inflow performance relationship while the tube hydraulics affect the outflow performance relationship. The computational model uses the nodal analysis method which is envisioned as a well-defined boundary value problem in mathematics. As such a third

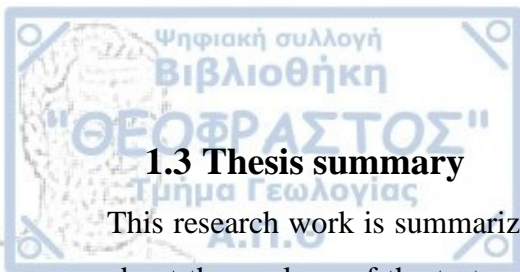
d.o.f was (iii) the average reservoir pressure suit for constructing various pumping scenarios to cover most test cases. To tackle this effort by considering a low average reservoir pressure \bar{p}_r equal with 4000 psi to a high average reservoir pressure \bar{p}_r equal with 9000 psi with a 500 psi step. With this pressure range it is easier to examine the behavior of the reservoir and its implications on the inflow performance relationship but also examine various factors influencing production that may require possible artificial lift methods in the future. Although artificial lift methods are out of the scope of this research, this work can serve as the basis for examining/investigating artificial lift methods (e.g., gas lift).

As with any other optimization problem, the factors affecting the problem can be quite a few, rendering the simulation inadequate. For this reason, we have constrained the problem by accepting a few assumptions based on optimum numerical convergence for more accurate simulation results. Also, one may note that there aren't many consistent data available for wellbore simulations and as such, the analyst is forced to consider assumptions to proceed with the simulations. The main assumptions considered in the modelling are listed in table 1.1 below.

Table 1.1: Simulation assumptions

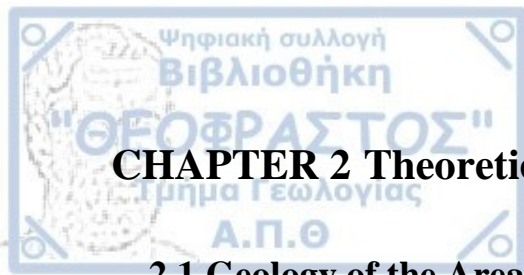
Gas specific gravity, SG_g , (-)	0.64
Heat transfer, h , (Btu/(h.degF.ft ²))	2
Drainage radius, r_e , (ft)	2000
Water specific gravity, SG_w , (-)	1.02
Contaminant Mole Fractions (no compositional change)	
CO ₂ Fraction, (%)	0
H ₂ S Fraction, (%)	0
N ₂ Fraction, (%)	0
H ₂ Fraction, (%)	0
CO Fraction, (%)	0

As explained above, the above values were chosen in such a way to ensure numerical stability for PipeSim software, in combination with lack of data where applicable. Additionally, this work could be extended if material balance data are obtained or made available through experiments in the future.



1.3 Thesis summary

This research work is summarized in four chapters. The second chapter provides information about the geology of the test area where the two wells are located. Also, it provides specific geological conditions that exist in the reservoir rocks where the wells were drilled. Finally, the fluid models (oil & gas) are also presented and all the necessary theoretical background about the equipment used for the completion of the two wells. In chapter three, the computational model is presented explaining the operational function of PipeSim software. Finally, chapter four presents the results from the simulations obtained. Additionally, in this chapter the main highlights and findings of this research work are presented and evaluated, along with some suggestions that can be considered as further work.



CHAPTER 2 Theoretical Background

2.1 Geology of the Area

The large Precambrian and Palaeozoic rocks of UK and Norway appear rarely as crops offshore, but under special cases when they do appear it is only for a small area of the order of few kilometres. Just outside the coasts of Northern England and Scotland, the Permian and Mesozoic outcrop appearing, is younger as compared to its part appearing onshore, with its base-Permo-Triassic outcrop pattern mimicking the coastline. Farther offshore, these strata are overlain by a post-rift caprock of Palaeogene and Neogene sediments that thickens towards the graben at the centre of the North Sea. Around the Moray firth coast, the outcropping Mesozoic strata are faulted and in contact with older rocks, and an extensive cover rock of the Cretaceous period exist. Off the coast of Norway, the band of Permian to Paleocene outcrop bordering the land is narrow as younger Palaeogene and Neogene strata occur relatively close to the coast (Copestake et al., 2003).

2.1.1 Geology of the North Sea

The North Sea is a continental sea with water depths which are generally less than 200 meters, although glacial erosion has created deeper waters in the extensive Norwegian channel that leads northwards into the Norwegian Basin. The continental break-of-slope to the Norwegian Basin is evident only in the far North (Copestake et al., 2003).

On the seabed, there is commonly a veneer of Holocene superficial sediments above Pleistocene deposits that are up to 800 meters thick in the Central Graben. Finer-grain Holocene and post-glacial sediments have mainly been deposited in the deeper waters, although there are also occurrences in local shallow in most coastal regions. Coarser-grained Holocene deposits are found on banks and towards the coast. Pre-Quaternary strata rarely appear as crops on coastal locations (Johnson, 2005).

In the Southern portion of the area, the seabed is generally smooth, sandy or slightly muddy, and less than 100 m in depth. In the far South and South-East of the Atlas area, waters become even shallower. Locally, deep channels exist such as the Devil's Hole, and towards the UK coast there are shallow banks that are of glacial origin and are covered by coarser grain sands and gravels. Farther North in the Witch Ground region, there are clay sediments in deeper waters with sands and gravels on the banks (Smith et al., 1994).

The Norwegian Channel sweeps around the Norwegian coastline and has water depths commonly more than 300 m, increasing to over 400 m in the North. The seabed in this characteristically steeply flanked channel is characterised by muddy sediments with abundant pockmarks (Hovland, 1983). For the readers knowledge, a pockmark is a depression or indentation on the Earth's surface, typically found on the seafloor but also occasionally on land. Pockmarks are often characterized by their circular to oval shape and can vary in size from a few meters to hundreds of meters in diameter and from centimetres to meters in depth.

The distribution of the oil and gas fields in the Atlas area shows that they are concentrated along the central zone of the North Sea, with a branch into the Moray firth region. This is because a three-arm graben system was developed, principally during the Late Jurassic. This rift structure has controlled many aspects of the petroleum geology of the region. The highly organic Kimmeridge Clay Formation that was deposited during the Late Jurassic has provided the required organic source for most oil and gas fields, and both the distribution and burial history of this formation has been controlled by the structural developments associated with the graben rift and post-rift subsidence. The structures that host the hydrocarbons are many and vary, but are directly related to the rift history and in particular the large and faulted blocks of the Viking Graben that were formed during the main rifting phases (Copestake et al., 2003).

During the syn- and post-rift development of the basin, many important episodes of clastic material were deposited in deep-water creating thick sandstone rocks in the rift, creating appropriate conditions for many reservoirs to be created and luckily to be sealed by the deepwater clay rocks surrounding these reservoirs. Post-rift subsidence observed in the centre of the main graben, with over 5 km of post-Jurassic sediments deposited extensively in many areas. However, this pattern is not reflected in the present-day bathymetry as the earlier basin configuration has been largely filled with Plio-Pleistocene deposits. Furthermore, Quaternary glaciers have eroded the relatively deep Norwegian Channel, close to the Norwegian coast, that gives a recently acquired asymmetry to the basin topography (Copestake et al., 2003).

2.1.2 Geology in the proximal area of the wells under study

In this subsection we describe the stratigraphy that was drilled to the total vertical depth (TVD). Most of this information is obtained from the *Norwegian Petroleum Directorate*. The first well under consideration (namely "well 6507/7-16 S") was drilled to test the Canela Beta prospect west of the Heidrun field on the Revfallet fault complex in the Norwegian sea.

The first lithostratigraphic unit is the *Norland group* together with *Naust formation*, both located at a depth of 371 meters. The Norland group is dominated by marine claystone

and is aged between middle to recent Miocene. The base of *Naust formation* has not yet been defined. The precise thickness is therefore unknown, but generally the *Naust formation* is several hundred meters thick in the Haltenbanken-Traenabanken area. It consists of interbedded claystone, siltstone, and sand, occasionally with very coarse clastic material in the upper part and its age can be dated in the late Pliocene.

The next underlying formation is the so-called *Kai*. It is 271 meters thick, and it consists of claystone, siltstone and sandstone with limestone stringers. In this formation, it is common to find Glauconite, pyrite and shell fragments with age ranging from early to late Miocene.

The *Hordaland group* follows at 1831 meters depth having an average thickness between 1100-1200 meters in the central and southern part of Viking graben, but in the Northern graben it only reaches a thickness of a few hundred meters. The group consists of marine claystones with minor sandstones. The claystones present a light grey to brown colour. Red and green claystones sometimes do appear but mainly at the formation base. Thin limestones and streaks of dolomite are also present. Sandstones are developed at various levels within the group. They are generally very fine to medium grained sized and are often interbedded with claystones. The group has a geologic age ranging between Eocene to Early Miocene. The immediate formation is *Brygge* located at the same depth 1831 meters and is in contact with *Hordaland group* formation. It is mainly composed from claystone with stringers of sandstone, siltstone, limestone, and marl. In this sandstone formation, pyrite, glauconite and shell fragments are common. This formation is aged between early Eocene to early Miocene.

The deeper formation is *Rogaland group* which is located at 2061 meters. In the west part of the formation, the dominant lithologies are sandstones interbedded with shales. These sandstones form lobes which pass laterally into shales eastwards, and in most of the Norwegian sector the *Rogaland group* consists of clay marine sediments. The basal deposits frequently contain reworked limestones and marls. Towards the top of this group, shales present a change in the texture towards tuffs. In the North Sea, its geologic age ranges between Palaeocene to early Eocene. As previously, at the same depth, *Tare formation* exists. It comprises of dark grey, green, and brown claystones with some thin sandstone stringers. It is just 58 meters thick and its age can be dated as late Paleocene.

The *Tang formation* which is located at 2096 meters depth has a thickness of about 72 meters. The formation lithology is described by dark grey to brown claystone with minor sandstone and limestone present. Its geological age ranges from Danian to late Paleocene. Minor amounts of sandstones are also present in the lower part in the Agat discovery area of *block 35/3*. The shales and sandstones in this formation are of calcareous type.

In the Maastrichtian sequence, the quantity of limestones is generally higher on the Horda Platform than in the Viking Graben. In the North Sea, the group ranges in geological age from Cenomanian to Danian.

The following formation is *Springar* which is located at 2163 meters and placed directly below the *Tang formation*. The siliciclastic facies of *Springar formation* are constrained in age to the Late Cretaceous period. It has a thickness, after verified by drilling, of about 167 meters and it comprises mostly from claystones interbedded with stringers of carbonates and sandstone. The formation age of this is Campanian to Maastrichtian.

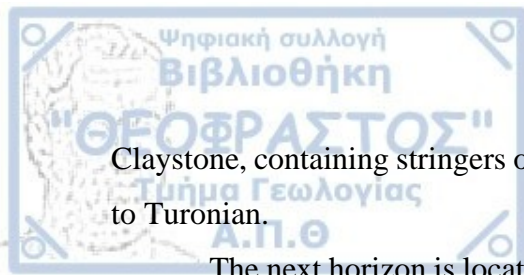
At larger depths the *Nise formation* is located at 2297 meters with a thickness of 212 meters, as verified by drilling. This formation is dominated by claystone interbedded again with carbonate and sandstone stringers. Its geological age is Santonian to Campanian.

Moving deeper, the *Kvitnos formation* is found at 2507 meters depth with a thickness of about 517 meters (verified by drilling), and it consists of calcareous grey and greyish claystones with carbonate and sandstone stringers. Its geological age is from Turonian to Santonian.

The *Cromer Knoll group* and *Lysing formation* are both met at 2774 meters depth. The thickness of the *Cromer Knoll* rock group varies considerably since the sediments were deposited in response to an active Late Jurassic tectonic phase. In the Viking Graben, the Åsta Graben and locally in the Central Trough, the thickness is more than 600 m but gradually thins towards the basin margins. The *Cromer Knoll Group* consists mainly of fine-grained, clay, marine sediments with a varying content of calcareous material. Calcareous claystones, siltstones, and marlstones are dominant rocks, but subordinate layers of limestone and sandstone occur. The claystones have various colours ranging from light to dark grey, olive-grey, greenish, and brownish. On the other hand, marlstones present a light grey, light greenish-grey, and light olive-grey colour. Few common minerals include mica, pyrite, and glauconite. In general, marlstones are the dominant lithology in both, upper and lower parts of the *Cromer Knoll group*. Its geological age ranges from Ryazanian to Albian - early Cenomanian in the North Sea and Ryazanian to Turonian in the Norwegian Sea.

Lysing formation lies between 2774m (upper boundary) and 2783m (lower boundary) giving just 17.5 meters thickness but verified by drilling. The formation lithology consists of sandstones, partly carbonate-cemented and interbedded with shales. The formation's age is between Late Cenomanian to Turonian or Coniacian.

Below the *Lysing formation*, at depth of 2783 meters, *Lange formation* has a thickness of 685 meters as verified by drilling. The dominant material comprising this formation is



Claystone, containing stringers of carbonates and sandstones with geological age of Ryazanian to Turonian.

The next horizon is located at 2967 meters and is the **Fangst group** together with **Garn formation**. The **Fangst group** typically comprises from three lithological units as follows: (i) a lower fine to medium-grained sandstone with numerous shaly interbeds, (ii) a middle mudstone and (iii) an upper relatively massive fine to coarse-grained sandstone. The **Garn Formation** consists of medium to coarse-grained, moderately to well-sorted sandstones. Mica-rich zones are also present. The sandstone is occasionally carbonate-cemented with a thickness of 45 meters. The geological age of **Fangst group** is dated from late Toarcian to Bathonian while the age of **Garn formation** is Bajocian to Bathonian.

At about 2993 meters from the seabed the **“NOT” formation** is found. The **“NOT” formation** consists of claystones with micronodular pyrite which coarsens upwards into bioturbated fine-grained sandstones which locally are mica-rich and carbonate-cemented presenting a thickness of about 37 meters and with age ranging from Aelenian to Bajocian.

Exciding the depth of 3000 meters, **Ile formation** has a 72 meters thickness with lithology consisting of fine to medium and in few occasions coarse-grained sandstones with various coarse grain sorting, interbedded with coarse grained but thin laminated siltstones and shales. In this formation, mica-rich intervals are considered to be common. Also, thin carbonate-cemented stringers appear, particularly in the lower parts of the unit and this formation presents a geologic age between Late Toarcian to Aelenian.

Moving on to 3090 meters depth, the **BAT group** is placed together with **ROR formation**. The average thickness of **BAT group** is 707 meters (considerably thick formation), and it consists of alternating sandstone and shale/siltstone units, with sandstone being the dominant rock in this formation. Its geological age is from Rhaetian to Toarcian.

At “target” depth, **ROR formation** lays next to the “pay zone” and has a thickness of 104 meters with geologic age ranging between Pliensbachian to Toarcian. The dominant fine-grained material is grey to dark-grey mudstones containing interbedded silt and sand with an increasing coarsening texture upwards, typically of few metres thick. Such sequences become more frequent towards the top of the formation, giving the unit an overall coarsening texture upwards which is a trend over most of **Haltenbanken formation**.

Lastly, the “pay-zone” formation is located at 3187 meters and is the well-known **Tilje formation**. It has a thickness of 91 meters (intermediate reservoir thickness) with a geologic age ranging between Sinemurian and Pliensbachian. The texture of this formation is very fine to coarse-grained sandstones which are interbedded with shales and siltstones providing an

excellent porosity as storage capacity of the reservoir. The sandstones are moderately sorted within the rock presenting great permeability for reservoir fluid transmissibility, however, with a high clay content as most beds are bioturbated. Finally, shale clasts and coaly plant remains comprise the upper layers of the pay-zone having finer grain interbeds of silt providing a good caprock for constraining the further movement of reservoir fluids and create conditions for accumulation. (<https://factpages.npd.no/>)

2.2 Reservoir Rock and Fluid Model

The hydrocarbons produced in the Norwegian sea are mainly Oil, that presents some special characteristics that makes it different from other types of hydrocarbons. The purpose of “well 6507/7-16 S” was to elucidate if there are any hydrocarbons inside the Garn formation, which as explained in the previous section belongs to the “Fangst” reservoir at the Heidrun oil field. The data pertaining to the reservoir rock used in the simulations are presented in Table 2.1. These parameters include: (a) geometry (thickness, well diameter and drainage radius), (b) petrophysical parameters (porosity, permeability, water saturation oil column thickness) and (c) pressure & temperature conditions in the reservoir rock (Theuerkorn, 2012).

Table 2.1: Fangst reservoir rock properties (Theuerkorn, 2012)

Parameter	Values
Reservoir thickness, d (ft)	295
Average porosity, Φ (%)	29
Range of field permeability, k (md)	670-19500
Average used in simulations, k (md)	1450
Oil column, h (m)	195
Average reservoir pressure, P_r (psi)	6500
Average reservoir temperature, T_r ($^{\circ}$ F)	176
Well diameter, r_w (inch)	10
Drainage radius, r_e (ft)	2000

In the following, Table 2.2 presents the reservoir fluid properties which include: the API gravity, the gas to oil ratio, the gas cap, gas and water specific gravity and finally the water cut range that was considered. At this point it important to note that we did not have sufficient data

for the water cut and we have treated this variable as a degree of freedom by performing simulations with 0% up to 35% considering a 5% step each time.

Table 2.2: Fangst reservoir fluid properties (Theuerkorn, 2012)

Parameter	Values
API gravity (⁰)	29
Gas oil Ratio, GOR (std ft ³ /STB)	628
Gas cap (-)	yes
Specific gravity of gas, SG_g (-)	0.6636
Water specific gravity, SG_w (-)	1.02
Water cut range	0-35

For completeness, we have assumed: (a) the Vasquez & Beggs correlation for the viscosity for the case of an undersaturated oil (e.g no gas considered initially), (b) the Chew & Connally correlation for the live oil and (c) the Beggs & Robinson correlation for the dead oil (PipeSim user manual, 2017). The above parameters were used to build the Rock and Fluid model in PipeSim software. By examining the parameters in Tables 2.1 & 2.2, it is seen that these are typical for a sandstone reservoir.

Porosity is considered as one of the essential parameters in modelling hydrocarbon recovery. The reason is that it controls the fluid storage capacity in the reservoir rocks, and their connectivity in the pore structure control the way fluids will flow and transported through geological formations. At this point it is considered important to mention that their relationship between the properties of individual minerals and the bulk properties of the rock should not be neglected in the modelling. Porosity is a rather easy variable to define, but certainly not easy to quantify. There are two types of porosity, the “*effective*” or open porosity that quantifies the recoverable volumes of fluids (any type) and the “*ineffective*” or closed porosity that constrains the recoverable quantities. In other words, a significant amount of hydrocarbons may be present but can only be recovered at some extent. For most reservoir rocks, porosity varies between 13% and 28%. The rock classification characterizing whether a reservoir rock has good storage capacity or poor is shown in Table 2.3 (Theuerkorn, 2012).

According to Table 2.3, the porosity of the Fangst reservoir can be characterized as **very good** and will provide excellent hydrocarbon reserves.

Table 2.3: Porosity characterization (Theuerkorn, 2012).

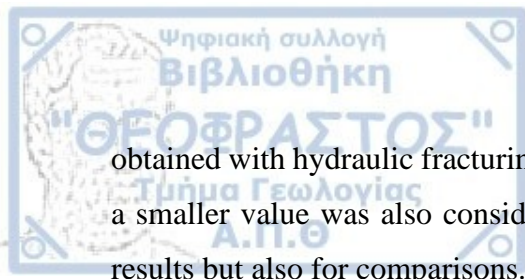
Percentage (%)	Characterization
0-5	Negligible
5-10	Poor
10-15	Fair
15-20	Good
20-25	Very good

Permeability is the other essential parameter which is of high importance in the modelling hydrocarbon recovery. This rock property of the porous material determines the ability of the fluid to flow through the porous medium. In other words, it expresses the flow capacity or the transmissibility of fluids. Without sufficient formation permeability, optimal hydrocarbon flow is not possible. Although permeability presents power law dependence with power law index (n) ranging from 4 (Timur correlation) to 6 (Morris-Biggs correlation), many factors can affect permeability. Any textural and geologic factors may increase or decrease the cross-sectional area of the permeating fluid affecting the permeating velocity and in turn the permeability via Darcy's law. The size of the grains in porous medium, their shape, and their sorting all can impact the space (hence the cross-sectional area of the permeating fluid) between grains thus influencing the material transmissibility. Table 2.4 shows a classification characterizing the reservoir rock transmissibility (Theuerkorn, 2012).

Table 2.4: Permeability characterization, (Theuerkorn, 2012).

Permeability values (md)	Characterization
1-10	Fair
10-100	Good
100-1000	Very Good

According to Table 2.4, the permeability of the Fangst reservoir can be characterized as very good, considering the fact that after well testing the range of the permeability is between 670-19500 md. In terms of modelling, the average permeability considered is 1450 md. It is important to note that no such permeability exists in nature for deep reservoirs but is achievable only after hydraulic fracturing. As such we considered this as a possible value since it can be



obtained with hydraulic fracturing. For completeness and for the purposes of the study though, a smaller value was also considered (250 md) to investigate its importance on the produced results but also for comparisons.

The API gravity is the term usually employed by the petroleum exploration and production sector to represent the fluid density. API unit is a way of determining the density of crude oil as compared with the density of water. If API unit is bigger than 10, then the crude oil is characterized as lighter than water, so it is able to float. On the other hand, if it is smaller than 10, then is characterized as heavier than water so it loses the float capability and it sinks. To describe API unit, physical units are not used, but it is reported in degrees. In general, crude oil with API between 40-45 is the most expensive because it can be considered the purest. For the Fangst reservoir, we have considered a 29 API unit oil density which falls in the medium density fluid. In terms of characterization, it is not the lightest but also not the heaviest (Filgueiras et al., 2014).

The Gas Oil ratio, or GOR, is the ratio of produced gas to produced oil. Typical units of GOR are SCF/STB. For the GOR=628 SCF/STB considered for the Fangst reservoir modelling, it means that 628 ft³ of gas are produced for every single barrel of oil. This is actually a big number, and it is affected from the oil, which is light in this case but also from the gas cap that exists in the reservoir. On the other hand, gas cap is the gas that accumulates in the upper portions of a reservoir where the pressure, temperature and fluid characteristics are conducive to free gas. The energy provided by the expansion of the gas cap provides the primary drive mechanism for oil recovery in such circumstances (Georgakopoulos, 2020).

2.3 Wellbores Description

As explained earlier, both wells used for the simulations in this work are located in the Norwegian sea. Both wells have similar characteristics which makes the comparison possible. Of course, there is not a second well that is the same with another, therefore some differences exist and they will be discussed in the following sections. The geological characteristics are also similar providing a better view and comparison giving the opportunity for easy and accurate simulations.

2.3.1 Reference well 6507/7-16 S

The reference “well 6507/7-16 S”, is located in the Norwegian sea. It is an exploration well, which started in 28/10/2019 and ended in 18/12/2019. Its produced products were oil and gas,

but it was plugged and abandoned for reasons we could not retrieve in the reports and in the literature. Therefore, its rock and fluid data are mainly used for education purposes in order to construct models with the really available data. The primary objective of our simulation was to investigate the production of hydrocarbons from the Garn Formation where the well is located. The seawater depth from the sea surface is 339 meters and the total depth (TVD) of the drilled well is 3238 meters. The oldest formation is Tilje that the wellbore penetrated is of the early Jurassic period (<https://factpages.npd.no/>).



Figure 2.1: Location of the reference well (<https://factpages.npd.no/>)

2.3.2 Second reference well 31/3-3

The second reference well used for the purposes of this work was “*well 31/3-3*”, which was drilled in the central southern part of the block east of the Troll Field. The main objective for simulating this well was to test the hydrocarbons production from the upper Jurassic sandstone that belongs to the Sognefjord Formation. When the well was drilled, no hydrocarbons were recovered in and for this reason this well was also plugged and abandoned labelling the well as “*dry well*”.

In this work, we created two models simulating both reference wells in the spirit of comparisons. Then we have changed the completion of the reference “*well 6507/7-16 S*”, by adopting the completion from “*well 31/3-3*” that proofed to be more efficient in the comparisons. The difference here between the wells is that we test in a real well the completion

from an optimum well to determine if the production from the reference “well 6507/7-16 S” could be optimized by adopting the completion string facilities of “well 31/3-3”.

The geology around “well 31/3-3” is similar to the reference “well 6507/7-16 S”, as they are both at the same area and share many characteristics. Also, the fluid model remains the same. The geological structure in which the well was drilled, goes beyond the water-oil contact (WOC), although there was not any water contamination in the hydrocarbons (Final well report 31/3-3). Figure 2.2 presents the “well 31/3-3” position (East) and TVD (2137m) in the Troll field (Eiken and Tøndel, 2005).

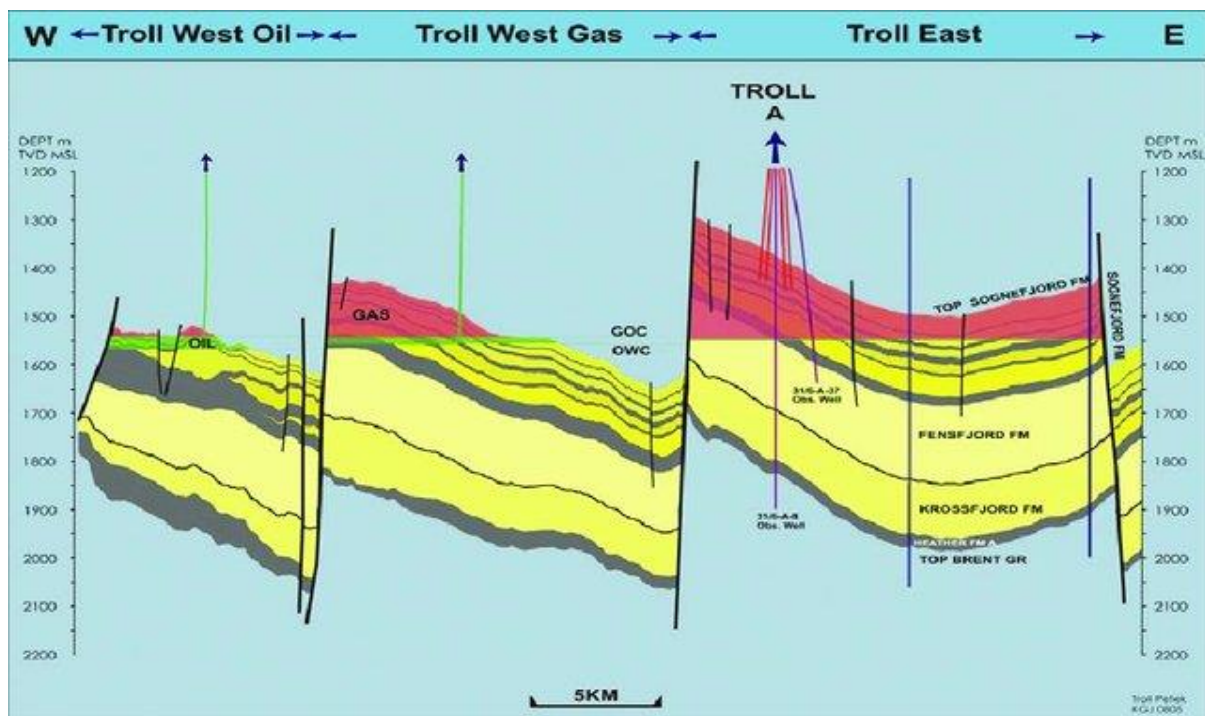


Figure 2.2: Wellbore position of “well 31/3-3” (Eiken and Tøndel, 2005)

As shown in Figure 2.2, the reservoir trap might be deeper than the water-oil contact, but the top of the Sognefjord formation extends above the water-oil contact, so the presence of water in the production phase is most likely not going to happen.

2.4 The Completion String Facilities

The scope of the completion varies between many reasons. Completions can be envisioned as the interference between the reservoir and the surface production. The completion string facilities are used as pressure management devices to handle the pressure from the reservoir, in a safe manner, towards the separator at the surface. The completion designer must complete a

drilled well and his design must ensure the flow of hydrocarbons safely and efficiently to the surface through the highly productive conduit that was created from drilling.

The completion starts with establishing the way that the well will be opened to flow or the establishment of the well and reservoir communication. This is done by the so called “*bottom hole completion techniques (bhct)*”. As soon as the well-reservoir communication is established, appropriate “*flow conduit*” must be selected and installed inside the well. The flow conduit is part of the “*completion string facilities*” or a.k.a “*jewellery*”. As soon as the completion string facilities are selected, are composed and lowered slowly in the open hole of the well and docked on the *tube hanger* at the top side of the well. Then the *Christmas tree* a.k.a “*x-mass tree*” is mounded on top of the tube hanger constituting the *well-head* of the wellbore. Then it is safe to conclude that the completion is now complete. Figure 2.3 presents the conceptual flow chart followed in well construction and completion design (Bellarby, 2009; Wan, 2011; Watt, 2014)

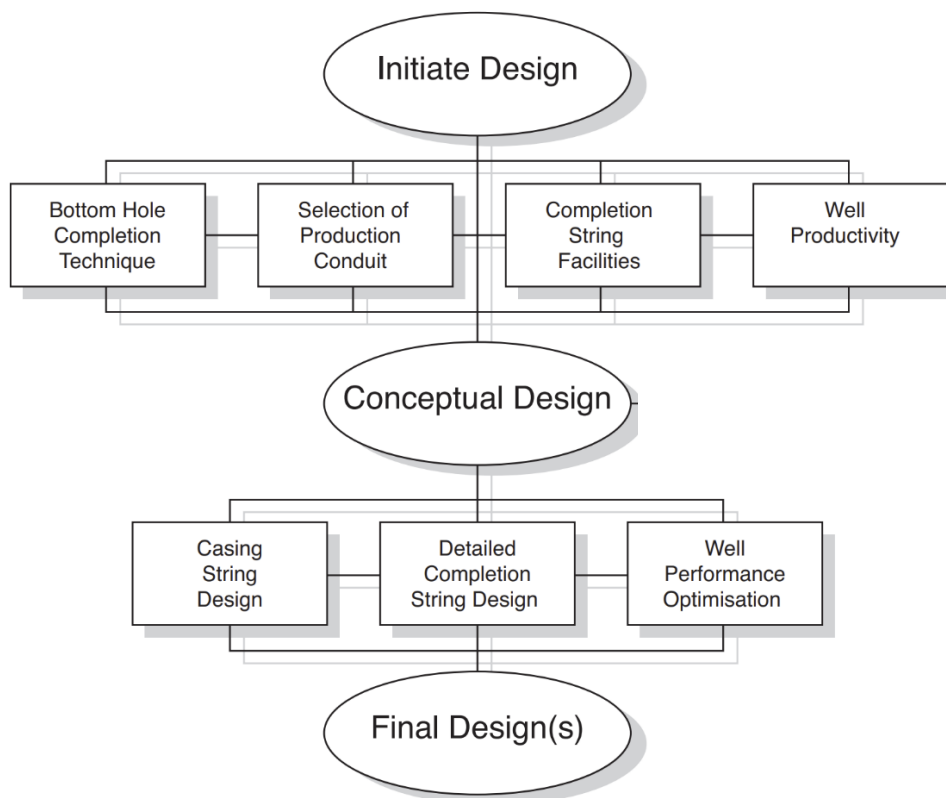


Figure 2.3 Well construction and completion design flow chart (Watt, 2014)

In the following sections we describe the basic five essentials of a conventional completion string. It should be noted that a completion string depends on many parameters and specialized conditions of the produced fluids and type of rock reservoir and their description is out of the

scope of our analysis. Figure 2.4 shows the location and the names of the basic completion string facilities. This equipment is used for managing the pressure from the reservoir to the surface and to ensure stable flow of hydrocarbons to the surface.

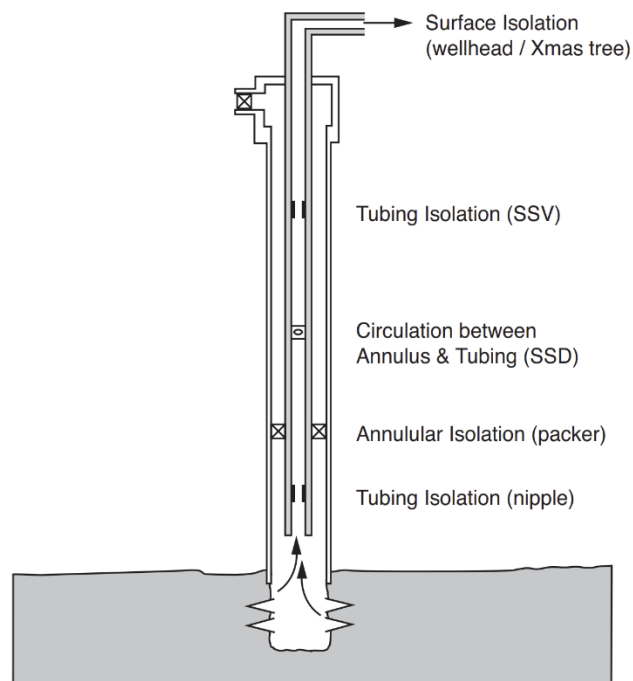


Figure 2.4: Basic well completion string equipment (Watt, 2014)

2.4.1 Landing nipples

Starting from the lower side of the completion string, a landing nipple is an accessory of the tube. It is placed inside the tube (internal profile) and used for multiple functions like secure a mandrel run either by wireline or by coiled tubing for pressure sealing and flow regulation. Many times, it is used as an entry point of hydrocarbons in the completion string. Functional wise, it provides: tube isolation for well shut-in or workovers, communication between the tube and the annulus, provides capability of remote control, regulates flow and used for pressure and temperature recordings (Watt, 2014). Figure 2.5 presents the schematic of a landing nipple.



Figure 2.5 Landing nipple (ruifengpetrotech-en.com)

2.4.2 Packers

Packers are downhole devices used to create isolation both vertically and horizontally. First, vertically is placed just above the production zone and secondly, between the tubing and the casing. These devices have a small diameter when they are run in a hole but later when the target depth is reached, they expand and push against the casing to provide isolation after applying an appropriate settling mechanism (e.g pressure or weight). There are two main types of Packers, namely the permanent and retrievable. Permanent packers are used in operations that don't require immediate packer removal. They provide better sealing than retrievable packers and are usually cheaper. If required, permanent packers can be removed by milling with coiled tubing. Usually, in high-temperature and high-pressure wells (LPLT) the permanent packers are preferred. Retrievable packers can be easily removed and reused by applying an external force to unsettle them. They are often used for well-intervention operations where specific zones must be isolated multiple times during the operation.

The main function of packers is to prevent reservoir fluids coming in contact with the casing because they can be highly corrosive and usually rich in CO₂ and H₂S causing corrosion damage on the well. Packers can also be used for other well completion operations such as hydraulic fracturing or matrix acidizing. (Bellarby 2009; Wan 2011; Watt 2014). Figure 2.6 shows an elastomer packer as part of the completion string.



Figure 2.6 Elastomer Packer (Bellarby, 2009)

2.4.3 Sliding sleeves (SSD)

Sliding sleeves are assembled as part of the completion string to establish communication between the tube and the annulus for single- or multiple- completions. Among its most important functions is the equalization of pressure between an isolated formation and the completion string, spot acidizing and fracturing, killing a well and directing the flow from the casing to the tubing in alternate or selective completions. Sleeves are available with various metallurgies and collaborate with a selection of landing nipple profiles. Sliding sleeves are handled by wireline locks and use nipple profiles. SSDs generally consist of a top sub, bottom sub, outer housing, and a sliding sleeve. Sliding sleeves are located above packer for circulation purposes or equalizing tubing or annulus before changing gas lift valves. If they are placed between packers then they serve production purposes or killing and stimulation purposes. (Bellarby 2009; Wan 2011; Watt 2014). Figure 2.7 show an SSD in open and closed mode.



Figure 2.7 Slide side door (SSD). (a) Open, (b) closed (Bellarby, 2009)

2.4.4 Subsurface Safety Valve (SSSV)

Just below the well head and at the highest parts of the well, a safety device is installed to provide an immediate shut-down of the producing conduits in the event of an emergency. Two types of subsurface safety valve are available. Namely, the surface-controlled (ScSSSV) and subsurface controlled (SSSV). In each case, the safety-valve system is designed to be the fail-safe, so that the wellbore can be isolated in the event of system failure or damage. Safety valves are designed to automatically shut in the flow of a well in the event of an emergency but also if surface controlled if the automatic shut-down fails. In practice, is mandatory, to have a secondary means of closure, for safety, for all wells that flow to the surface. (Bellarby 2009; Wan 2011; Watt 2014). Figure 2.8 presents a Sub Surface Safety Valve (SSSV).

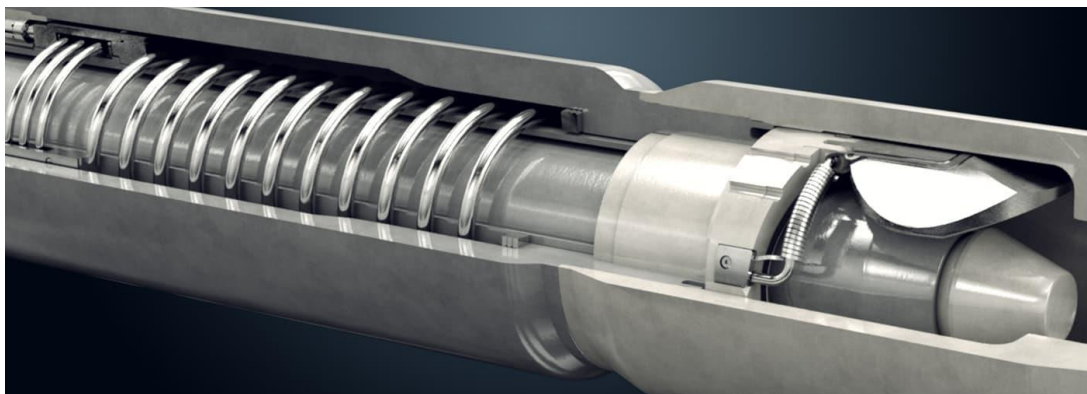


Figure 2.8 Sub Surface Safety Valve (SSSV) (superiorenergy.com)

2.4.5 Wellhead assembly

The wellhead assembly provides the outmost top equipment used to seal the well and direct hydrocarbons to the separator. Usually, it comprises from the tube hanger and the Christmas tree (X-mass tree). The wellhead assembly is very important for the completion string because

(a) suspends all casings and tubulars, (b) enables the installation of a surface flow control device on top of the well (e.g., blow-out preventer) and (c) provides hydraulic access to the annulus between the production casing and tube for fluid circulation. The X-mas tree on top of the wellhead, is a system of valves providing flow control of the produced or injected fluids. It is normally installed on top of the wellhead after the installation of the production tubing constituting the wellhead assembly (Watt, 2014). Figure 2.9 (a) shows a section of a wellhead and (b) the Christmas tree.

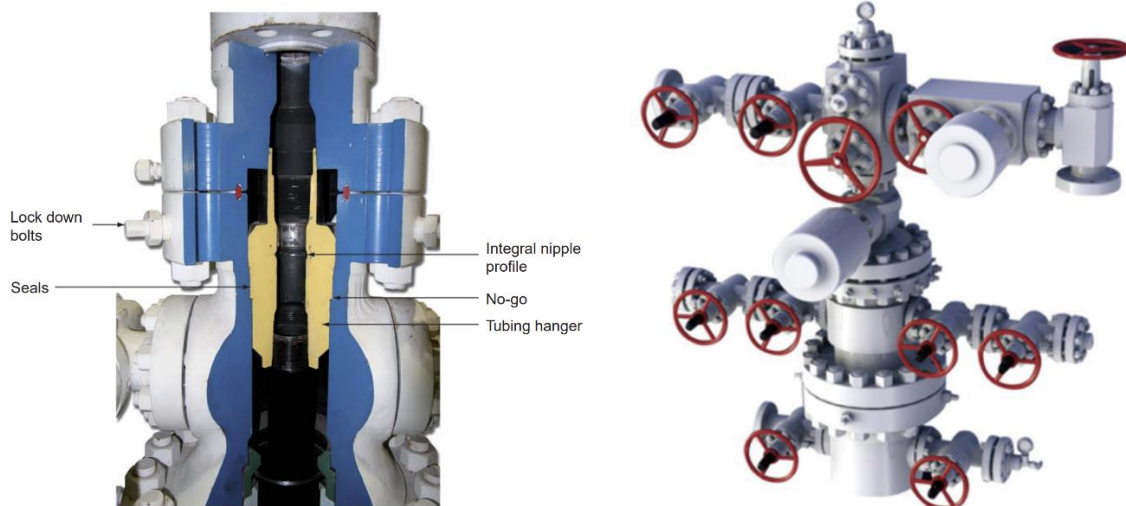


Figure 2.9 (a) Wellhead section and (b) X-mas tree (a: Bellarby 2009; b: camtop-oilfieldtools.com)

2.5 Nodal Analysis

Nodal analysis in the context of petroleum simulations refers to a mathematical and computational technique used in the modeling and simulation of oil and gas reservoirs either with commercial software or with self-constructed numerical codes. It is one of the fundamental methods for understanding the flow of fluids (e.g., oil, gas, and water) within a reservoir and optimizing production strategies. Nodal analysis can be used in power system analysis, which involves transforming the network into a simplified model for analysis. The radial equivalent independent (REI) model is a commonly used approach, which represents the network as a circuit. By using computers, the user can manipulate and solve these models for providing valuable insights. A typical simulation with nodal analysis includes:

Reservoir Representation: For petroleum applications, reservoirs are typically represented as a network of nodes and connecting pathways, similar to an electrical circuit. Each node represents a point within the reservoir, which may include wellbores, fractures, or specific grid blocks in a numerical reservoir model. **Flow Equations:** By using nodal analysis the flow equations that describe how fluids move within the reservoir can be solved. These flow

equations are typically variants of Darcy's law, which govern fluid flow through porous media. It is reminded that key parameters for solving a Darcian flow include permeability, porosity, fluid properties, and pressure differentials. **Nodal Equations:** As explained above, at each node in the reservoir model, a set of nodal equations are constructed based on the flow equations. These nodal equations relate (i) the pressures, (ii) flow rates, and (iii) saturations of the fluids at each node a.k.a degrees of freedom (D.O.F). The constructed nodal equations can describe efficiently the conservation of mass and momentum for each fluid phase (oil, gas, and water) within the reservoir. **Boundary Conditions:** to appropriately describe the system under consideration, appropriate boundary conditions must be assumed to account for the interactions between the reservoir and external systems, such as wellbores and surface facilities. These boundary conditions are crucial for the simulation of production or injection and how their physical process can affect the reservoir performance. **Solver Algorithms:** To solve the final system of nodal equations the user must apply numerical methods like finite differences or finite elements, or even finite volumes, depending on the specific characteristics of the reservoir under consideration for simulation.

After obtaining results for specific problems, poses only the first approach to the solution of the problem. After that the analyst must perform a series of simulations for **Production Optimization**. Once the nodal analysis is performed and the reservoir simulation is run, analysts can use the results to optimize production strategies. This includes decisions on (i) well placement, (ii) injection rates, (iii) production rates in order to maximize hydrocarbon recovery and economic profitability. Also, **Sensitivity Analysis** can be used involving the assessment of how changes in various reservoir parameters (e.g., permeability, porosity, well locations) can affect positively or inhibit reservoir performance. This information is valuable for making informed decisions during reservoir development and management. Finally, an **Uncertainty Analysis** can be performed alongside with nodal analysis to account for any uncertainties in reservoir parameters and improve decision-making under uncertainty (Dimo, 1975; (PipeSim user manual, 2017); Ahmed et al., 2023).

Further applications of Nodal analysis include the identification of the conditions under which a well may require artificial lift installations, along with the most efficient lift method to be used. Installing artificial lift equipment poses special challenges which only by simulations, the optimal position can be determined. The nodal analysis for this kind of problems aims to optimize the system to produce the target flow rate in the most cost-effective manner possible. Additionally, it seeks to evaluate each component in the well system to identify and eliminate any factors hindering flow rate. With nodal analysis, many wells can

continue their current or increase production rates which may not have been optimized or completed in a way that allows them to achieve their maximum potential rate without prior use of numerical simulations (Brown & Lea, 1985).

2.5.1 Well performance

The assessment of well performance can be obtained by means of the nodal analysis method. Well performance can be divided into two groups of analysis. The “*inflow*” that corresponds to attracting the fluids from the reservoir to the well and the “*outflow*” that corresponds to the *lifting* of fluids from downhole to the surface. Thus, the inflow and outflow performance of an oil well refers to the analysis and assessment of how fluids (primarily oil, gas, and water) move into and out of the wellbore. This analysis is crucial for modelling to understand the behavior of the reservoir and optimizing production (Watt, 2014; Bellarby, 2009; Wan, 2011).

The performance characteristics for the inflow begins with an understanding of the reservoir's behavior. This includes the reservoir's properties such as permeability, porosity, and fluid properties (e.g., viscosity) as well as the initial reservoir pressure. Then, the geometry and type of completion of the wellbore play a significant role in inflow performance. Factors such as the well's depth, diameter, and completion design (open-hole or cased-hole) impacts the communication of the well and the reservoir influencing fluid flux. Usually, the inflow of fluids into the wellbore is governed by Darcy's law, which describes how fluids flow through the porous reservoir formation. The quantification of the inflow performance is made with the help of a quantity called “*productivity index*” because it represents the ability of the reservoir to deliver fluids to the wellbore under a given set of boundary conditions also known as drawdown pressure ($d_p = P_r - P_w$), where P_r is the average pressure in the reservoir and P_w is the pressure conditions inside the well. The PI is often calculated with the help of Darcy's law and is expressed in units of flow rate per unit pressure drop (e.g., barrels per day per psi). Finally, the well performance can be determined with the help of the Inflow Performance Relationship (IPR). The IPR is a curve that illustrates the relationship between the well's production rate and the flowing bottomhole pressure (BHP). The IPR is the main available parameter for assessing any changes in production rate influence the drawdown (pressure drop) in the reservoir.

As soon as the IPR is constructed then the outflow performance must be determined. As explained earlier, the outflow performance analysis focuses on the behavior of fluids as they travel up the wellbore to the surface. This includes factors that are foreseen in the modelling the completion string and the equipments used. Also, wellhead pressure, tubing size, and surface facilities can influence the outflow performance. As fluids flow up the wellbore, usually

pressure drop is observed that us attributed mainly due to friction and the operating wellhead pressure P_{wh} . This pressure drop must be determined via simulations and controlled appropriately to ensure efficient production. In many oil wells, gas can also be produced along with oil and water. Proper facilities and equipment are required to separate and handle gas from the liquid phases. The choice of separation equipment (e.g., separators, compressors) impacts the outflow performance and are always part of the simulation and completion process. In some cases, especially for older wells or wells with declining reservoir pressure, artificial lift methods and equipment can be used to assist in the kinetic energy of the fluids travelling up the wellbore. Such equipment include electric submersible pumps (ESPs), rod pumps, or gas lift could be employed to enhance outflow performance. Also, the efficiency of the surface production facilities, including storage, separation, and transportation systems, are very important in ensuring constant and stable outflow performance. Finally, chokes placed at the wellhead allows operators to control the flow rate and optimize the pressure at the surface which is essential for managing outflow performance (Watt, 2014; Bellarby, 2009; Wan, 2011).

For predictions, when the inflow (specific for reservoir conditions) and outflow (specific for completion string selected) performance relationships are determined then are plotted together on a same graph. When doing so, an intersection point is observed which is called the operating point or (OP). This OP dictates the required operating pressure and the respective flow rate that will be produced. The OP is easily understood that is influenced by the type of completion string facilities selected. Figure 2.10 presents a typical example of how the OP is determined via the inflow and outflow performance relationships (Vo et al., 2020).

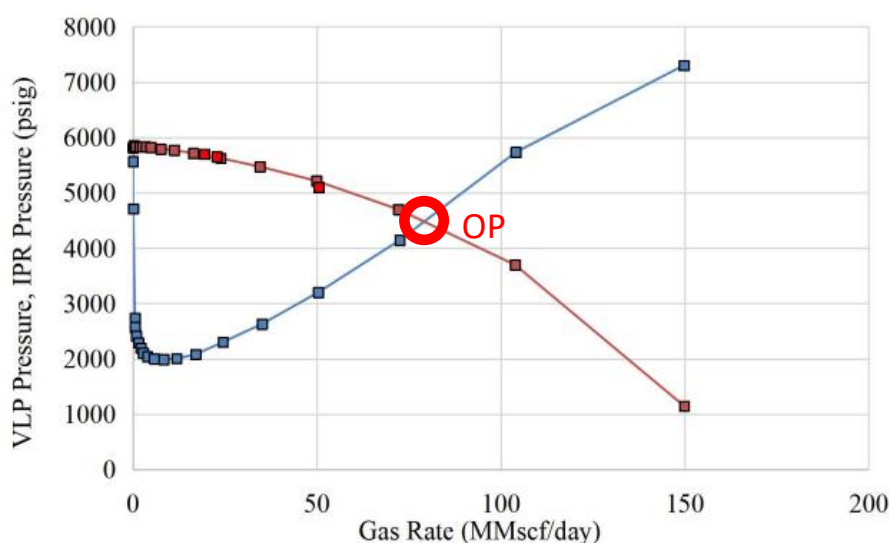
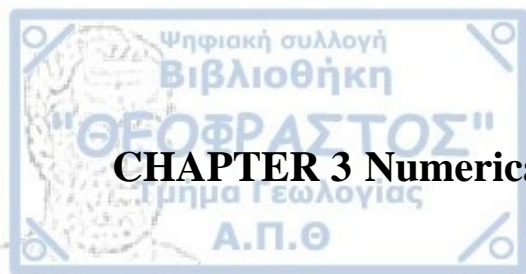


Figure 2.10 Typical inflow, outflow performance relationships with operating point for a gas reservoir (Vo et al., 2020)



CHAPTER 3 Numerical Simulations

3.1 PipeSim Software

For the purposes of this work, we have used the PipeSim software provided by “Next” company owned by Schlumberger. The PipeSim simulator offers the industry’s most comprehensive steady-state flow assurance workflows for front-end system design and production operations. As such, we have designed the two wells with this software to simulate the wells in actual conditions. The flow assurance capabilities of the simulator enable analysts to ensure safe and effective fluid transport—from sizing of facilities, pipelines, and lift systems, to ensuring effective liquids and solids management, to well and pipeline integrity. Shared heat transfer, multiphase flow, and fluid behaviour methodologies ensure data quality and consistency between the steady-state and transient analyses. Although, PipeSim is a very user-friendly software, its major limitation is that it cannot capture transient behaviour in the systems under consideration (PipeSim user manual, 2017).

3.2 Models Setup

For the reference well, all the data regarding the depth, sea, formations and equipment were obtained from wellbore “6507/7-16S” located at the Norwegian Sea. The information provided to the simulator, was not only for the well, but also for the production (i.e., how many barrels per day). As explained earlier, this particular well was characterized as plugged and abandoned (P&A), it was used as a reference well to investigate and optimize its production but also to apply the knowledge obtained from the simulations to another well to improve its production. In this hypothetical scenario, the production of the well is examined in different degrees of freedom (d.o.f), like (i) different tubing depths and (ii) dimensions and (iii) different equipment positioning. All these were examined in order to see their impact on the final production. Later on, the simulation results of this well were applied to another well with similar wellbore characteristics and evaluate its performance.

3.2.1 Description of modeling procedure

When prompt to start the simulator, PipeSim requests to declare the type of analysis. That is, a single well or a network of wells or combination of both. For the purpose of this study, we have selected the single well simulation. The workspace interface is shown in figure 3.1.

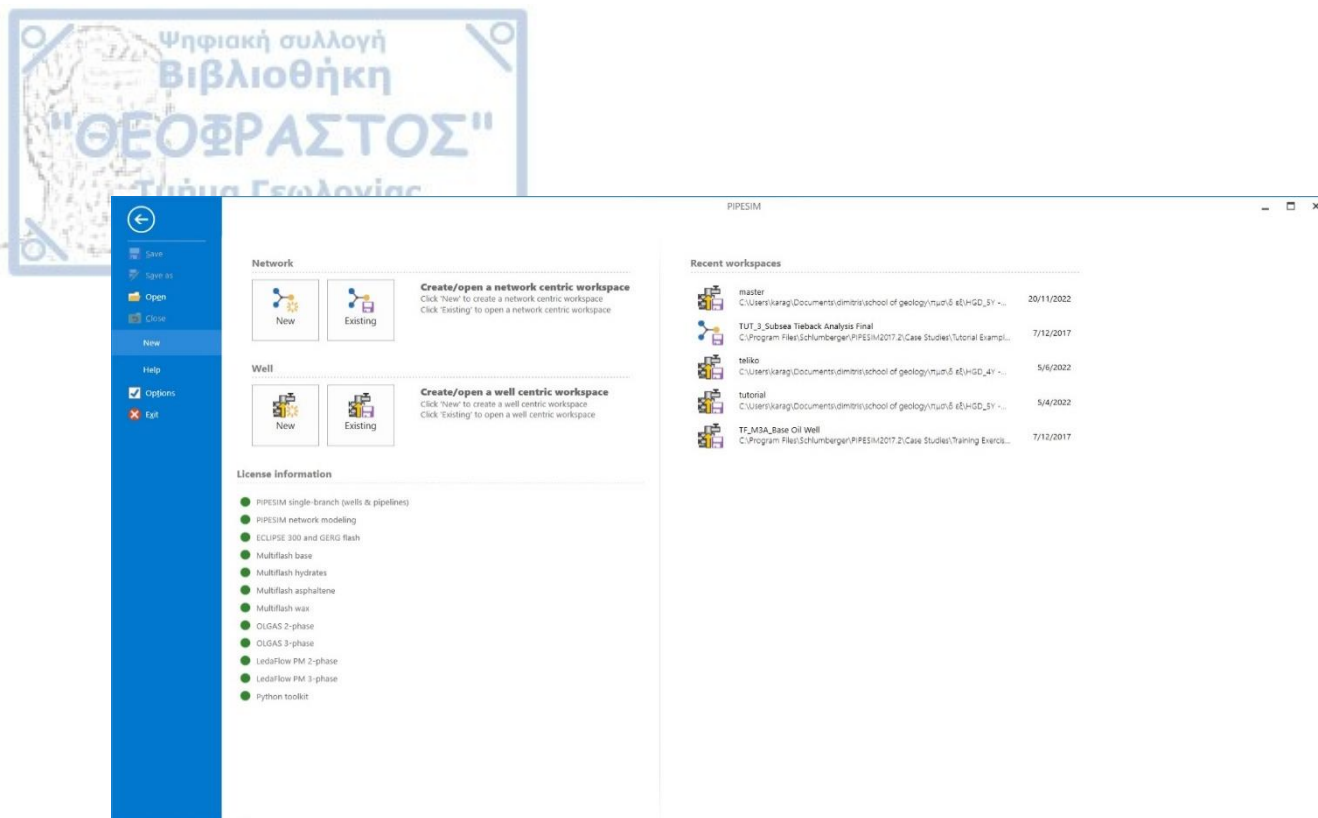


Figure 3.1: Pipesim workspace interface

The first requested input data needed are the name of the well, if it is active and what is the type of the well (i.e., injector or producer). For the purposes of this work, the simulated well is active, and it is a production well. An injection well is used to place fluid underground into porous geologic formations which is out of the scope of this analysis. Figure 3.2 show the tab where these data are inserted.

Well name:

Active:

Well type: Production Injection

Check valve setting:

Figure 3.2: General input data

The next step is to include the tubulars and its properties. To do so, the casing types and depths are given to the simulator. The material properties of the casing types are available through the libraries of PipeSim but no such information was given in the literature, so we considered the default option as a wise choice. For the modelling case, there were five stages of casing strings. Starting from the well-head, the first casing is the conductor pipe. **Conductor pipe** is a large diameter pipe set into the seabed to provide the initial stable structural foundation for a borehole or oil well. As the first string of casing, it's the largest diameter pipe installed in a well. Benefits

of conductor pipe include: keeping the hole from caving into the wellbore, protects natural materials from drilling fluids, supports surface casing and removes streamlines of drill cuttings suspended in drill mud. Also, it is often called the “*drive pipe*” because sometimes it’s driven into the ground with a pile driver. In offshore drilling applications, conductor pipe plays a pivotal role as a critical structural foundation element for subsea wellheads. (iadclexicon.org)

The next part of the casing string is the ***surface conductor casing***. This type of casing is used to protect shallow fresh water sands from possible contamination. Another important reason for installing this casing is to prevent cave-in of any unconsolidated, weak and near surface sediments. Also, it assists to flow containment with the help of a blowout preventer. Last, it is used to support and protect from corrosion any subsequent casing strings runned in the well. (gbpipemill.com)

Following the other two types of casings, the ***intermediate casing*** is installed. The two main purposes of this part of the casing string are like the surface casing. Its function is to permit the final depth to be reached safely and also to isolate problematic zones, for example any type of formations that have abnormal pressure, that may cause lost circulation, sloughing or caving zones between the surface casing depth and the production casing depth.

The final casing string is the ***production casing***, that extends from the surface to the final drilled depth. It is a critical component in the construction of an oil well. It is a certain diameter casing (depending on the design) that is inserted into the wellbore after the drilling process is complete. The primary purpose of production casing is to provide structural integrity to the well and to isolate the surrounding geological formations just before the communication between the reservoir rock and the well is established.

For final part of the well construction, it the so-called *bottom hole completion technique*. From the final well report this part of the well is done via a liner. A ***liner*** can be used in well construction to isolate problematic pay zones during production by screening-out sand particles which hydrocarbon production from sandstones are usually accompanied with. For some practitioners, a liner is considered as a different type of casing profile. One of the primary advantages of using liners is that it can be runned quickly, compared to other tubulars. A disadvantage of a liner is the previous casing string must withstand the pressures encountered after drilling below the liner which means a heavier design with a larger diameter casing.

For the purpose of this study, we have examined also two other different options. (a) the open hole (a.k.a. “*barefoot*”) and the other (b) cemented and perforated. This could create some difference in the production because the cross-sectional area of the fluid flux is significantly altered and according to Darcy’s law the flow rare is divided by the cross-sectional

area that fluid flux takes place. The open hole completion refers to the case where the oil reservoir is completely exposed during the completion of a vertical or horizontal well whereas the cemented and perforated refers to the case where the well is completely isolated from the reservoir and only small slots are created via shape charge guns (perforation guns) to pierce the casing, the cementing and some part of the rock (of the order of 1-2 meters). Figure 3.3 and 3.4 presents the tab where the well construction (geometry) and material data are inserted in the simulator for the barefoot and for the cemented and perforated cases respectively.

Mode: Simple Detailed
 Dimension option: OD Wall thickness

^ CASINGS/LINERS

	Section type	Name	From MD	To MD	ID	Wall thickness	Roughness	
			ft	ft	in	in	in	
1	Casing	conductor	0	1437,008	30	0,361	0,001	...
2	Casing	surf.cond	0	1942,257	20	0,2983471	0,001	...
3	Casing	interm	0	3946,85	13,375	0,2241526	0,001	...
4	Casing	liner	0	9635,827	9,625	0,1530992	0,001	...
5	Open hole	open hole	9635,827	10623,36	8,5			

+

^ TUBINGS

	Name	To MD	ID	Wall thickness	Roughness	
		ft	in	in	in	
1	Tubing	9636	2,375	0,425	0,001	...

+

Figure 3.3: Well construction (geometry) and material data for the case of barefoot

^ CASINGS/LINERS

	Section type	Name	From MD	To MD	ID	Wall thickness	Roughness	
			ft	ft	in	in	in	
1	Casing	conductor	0	1437,008	30	0,361	0,001	...
2	Casing	surf.cond	0	1942,257	20	0,2983471	0,001	...
3	Casing	interm	0	3946,85	13,375	0,2241526	0,001	...
4	Casing	liner	0	9635,827	9,625	0,1530992	0,001	...
5	Casing	casing	0	10623,36	8,5	0,09506258	0,001	...

+

^ TUBINGS

	Name	To MD	ID	Wall thickness	Roughness	
		ft	in	in	in	
1	Tubing	9636	4,5	0,425	0,001	...

+

Figure 3.4: Well construction (geometry) and material data for the case of cemented and perforated

After constructing the well, the next step is to select the equipment that will constitute the completion string. The first completion string facility is the tube requiring the depth, the internal diameter (ID) and material type which can vary, depending on the type of the simulation. For this specific model, different tubing depths and ID were examined as part of

the hydraulic parametric analysis performed, in order to optimize the final production. The selection of tube as the flow conduit from the bottom hole to the surface permits better well control and flow stability. Flow efficiency is typically improved with the use of tubing. Furthermore, tubing is required for most artificial lift installations. Tubing with the use of a packer allows isolation of the lower side of the well with the rest of the well by keeping well fluids in the lower side and avoiding corrosion damage of the casing. The tubing size was chosen by a Halliburton catalogue, along with the SSSV size. According to this catalogue, there are limits on the size of the safety valves, so they have to match with the tubing. The SSSV properties will be discussed in the next sections (Halliburton.com). Table 3.1 presents the tubing inner diameter sizes for the four different models created with variable well penetration depth.

Table 3.1: Penetration depth with various tubing sizes (Halliburton.com)

Well penetration depth (ft)	Tubing ID (inch)	
	9636	2-3/8
10123	2-7/8	2.875
10450	3-1/2	3.5
10450	4-1/2	4.5

Next the deviation survey tab is activated. In this tab the calculation options and the reference options are inserted. The well “6507/7-16S” is nearly vertical and aligns with the purpose of this analysis. For the reference options the wellhead depth is inserted at the seabed, which according to the report, is located at a depth of 339 m from the Rotary Kelly Bushing (RKB) but also the final depth is required which is transferred automatically by the previous tab after inserting the final casing depth. Figure 3.5 presents the tab for these definitions.

General | Tubulars | Deviation survey | Downhole equipment | Artificial lift | Heat transfer | Completions | Surface equipment

CALCULATION OPTIONS

Survey type: Vertical

REFERENCE OPTIONS

Depth reference: Original RKB

Wellhead depth: 339 m

Bottom depth: 10623,36 ft

Figure 3.5: Deviation survey

The next definition is related with the downhole equipment. The basic equipment used for the definition of the completion string are (i) the SSSV, (ii) the sliding sleeve and (iii) the packer. The size of the SSSVs is chosen together with the tubing size according to Haliburton's catalogue. The installation depth can be different according to several theories. Many scientists believe that they should be placed at some distance and just below the wellhead while others support that they should be placed deep in the wellbore. In this study, we adopted the first case where the SSSV was installed at about 385 ft below the wellhead. The sliding sleeve was placed also in a different position, deeper than the SSSV but higher than the packer. For optimum results a median depth was finally selected at 2921ft. Finally, the packer as in most completion cases are placed just above the reservoir providing zonal isolation which is 9136 ft. Figure 3.6 shows the input data for the downhole equipment tab.

General					Tubulars					Deviation survey					Downhole equipment				
		Equipment	Name	Active	MD														
					ft														
1	SSSV	SSSV	SSSV	<input checked="" type="checkbox"/>	1462,205														
2	Sliding sle...	Sleeve	Sleeve	<input type="checkbox"/>	4000														
3	Packer	Pk	Pk	<input checked="" type="checkbox"/>	10241,64														
4		NA	NA	<input checked="" type="checkbox"/>	11112,2														
+																			

Figure 3.6: Downhole equipment data

At this point it should be noted that for completeness we have examined the influence of varying the depth of the equipment (packers, sliding sleeves and SSSV) to reach optimum results. For presentation purposes we only present the ones that produced the optimum results (see Figure 3.6).

The definition in the simulator is artificial lift. The term Artificial lift refers to number of techniques and equipment used by the petroleum industry to assist the flow of hydrocarbons from downhole to the surface when the natural reservoir pressure is insufficient or depleted to lift the fluids to the surface. As a well ages, its natural reservoir pressure declines, making it necessary to use artificial lift methods to maintain or enhance production by providing the necessary kinetic energy to the fluid artificially (Brown, 1982). From examining the report, we did not come across to any data for artificial lift and for this reason (lack of data) the use of artificial methods was not considered and all artificial lift parameters were kept the default ones

(Specific gravity of gas equal with 0.64). Figure 3.7 presents the artificial lift tab and the default values considered in the simulations.

General Tubulars Deviation survey Downhole equipment **Artificial lift** Heat transfer Completions Surface equipment

GAS LIFT
Injection option: Fixed injection ports Injection valve system
Alhanati stability check:

Gas lift	Active	MD	Injection basis	Inj. quantity	Injection unit
		ft			

GAS PROPERTIES
Gas specific gravity: Specify Use fluid model

PUMP LIFT

Equipment	Name	Active	MD
			ft

Figure 3.7: Artificial lift tab (no artificial lift was simulated)

The required definition is related with heat transfer phenomena. The value of the overall heat transfer coefficient has assumed to be constant. Also, due to the lack of required data for the simulations, the default option was chosen once again. The only value changed was the soil temperature at wellhead. The wellhead is placed at a depth of 385 meters and the temperature is different deep in the ocean than in standard conditions on the surface. The average temperature is 39.2 °F or 4 °C. Figure 3.8 presents the heat transfer tab and the considered values for heat transfer in the simulations.

General Tubulars Deviation survey Downhole equipment Artificial lift **Heat transfer** Completions Surface equipment

U Value input: Single Multiple

Heat transfer coefficient: Btu/(h.degF.ft2)

Ambient temperature input: Single Multiple

Soil temperature at wellhead: degF

Figure 3.8: Heat transfer properties considered in the simulations

The following required definition is regarded with the reservoir and the fluid model all included in the completions tab. Here, the perforations parameters are also inserted. For the purpose of this study, we have considered that the perforations depth (for the case of cemented and perforated model) were placed at 11112 ft. The required pressure boundary condition of the reservoir was considered to be 6500 psia, the temperature condition was 176 °F, the IPR was considered to be linear. The reservoir has about 295 ft thickness with 1000 mD permeability (after hydraulic fracturing-stimulation). Finally, the borehole diameter equal to 10 in. The skin of the rock formation will be part of the sensitivity analysis and will be discussed in the following sections. Concluding, we have considered the black oil model for the fluid. Figure 3.9 presents the tab for the required data input pertaining to the completions.

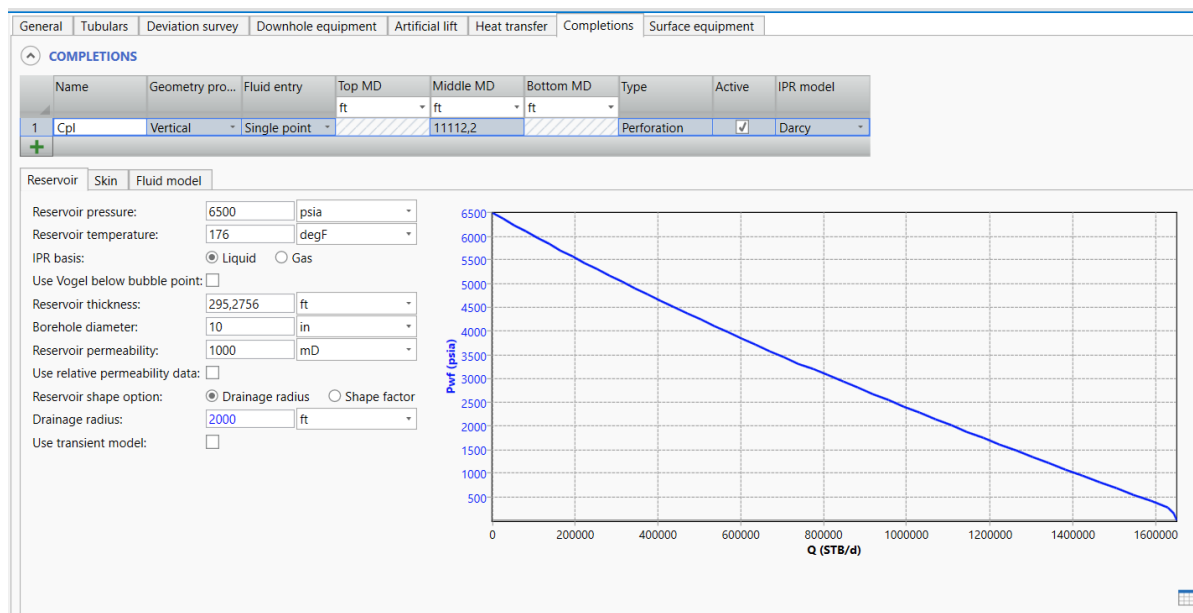


Figure 3.9: Completion tab properties (reservoir, fluid model and perforations)

In the following figure 3.10 we present the final well completion model that was constructed in PipeSim simulator. With Figure 3.10, we outline the detailed view of the equipment, and location with depth.

1079 ft

1112 ft

1437 ft

1942 ft

3947 ft

4000 ft

9136 ft

9636 ft

10450 ft

10600 ft

10623 ft

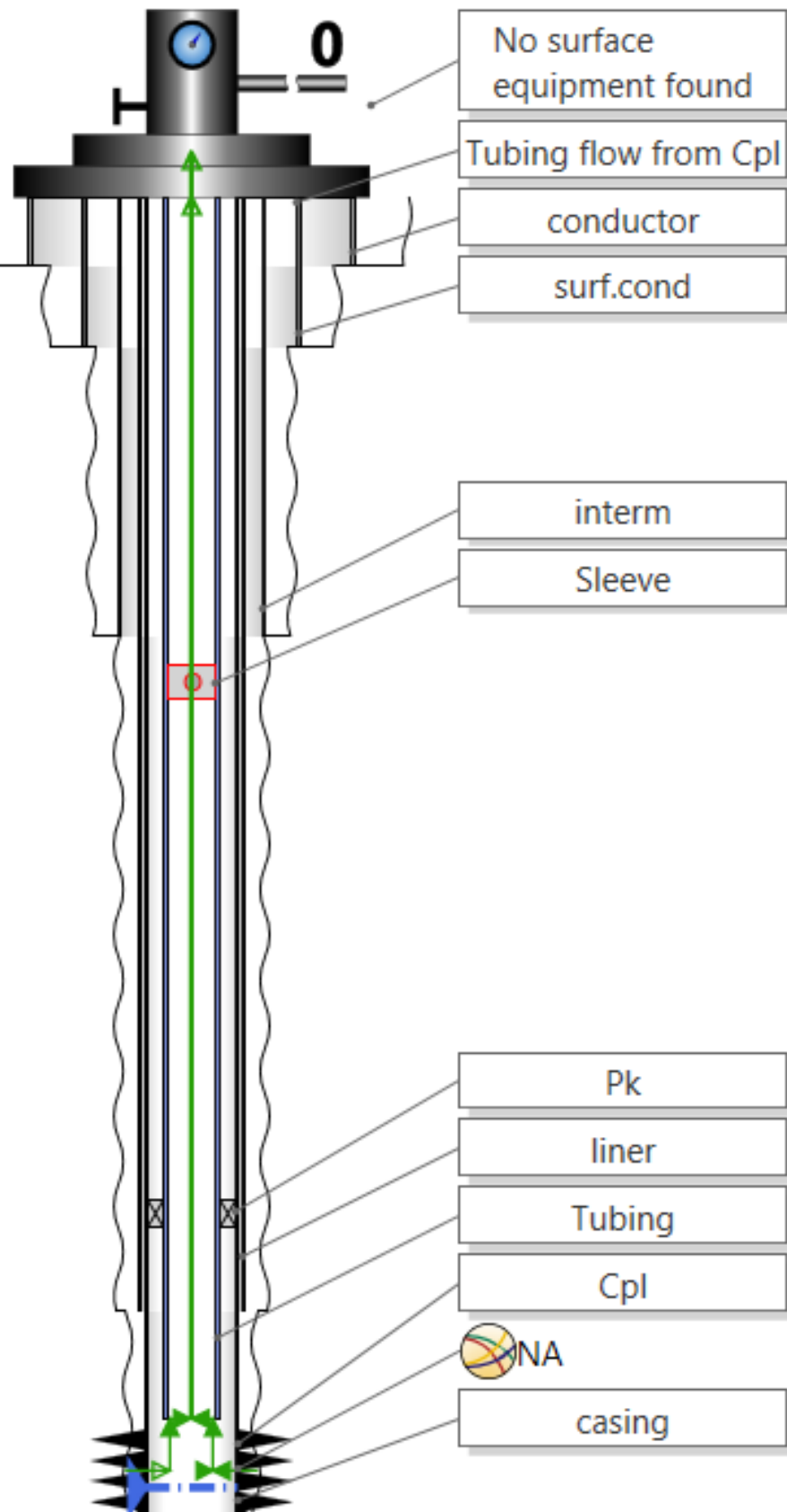


Figure 3.10: Final well completion model for "6507/7-16S"

3.2.2 Simulation results for the reference well “6507/7-16S”

In this section, the results for the reference well “6507/7-16S” are presented and the best-case scenarios are chosen. The main target, system-wise of the simulation analysis is to increase well rates by keeping constant the known variables and instigate parametrically the variables we do not have any data. We did not have any information about the pressure profiles and for this reason we have assumed a large pressure reservoir in order to forecast production in a more realistic way (PipeSim user manual, 2017). Therefore, we have examined production with a reservoir pressure ranging between 8500 psi and 4000 psi with 500 psi step. It should be noted that the reservoir pressure considered, $P_r = 6500$ psi serves as an initial value for numerical convergence. The resulting solution (and hence the well performance) is plotted in figures which are called inflow (IPR: Inflow Performance relationship) and outflow (TPC: Tube Performance Curve) performance graphs. The IPR is defined as the well flowing bottom-hole pressure (P_{wf}) as a function of production rate Q . It describes the flow from the reservoir to the well. The P_{wf} is defined in the pressure range between the average reservoir pressure and atmospheric pressure. The TPC, describes the bottom-hole pressure as a function of flow rate. The TPC depends on many factors including fluid PVT properties, well depth, tubing size, constructed material, surface pressure, water cut and GOR. Both the Inflow and outflow performance relate the wellbore flowing pressure to the surface production rate. (production-technology.org).

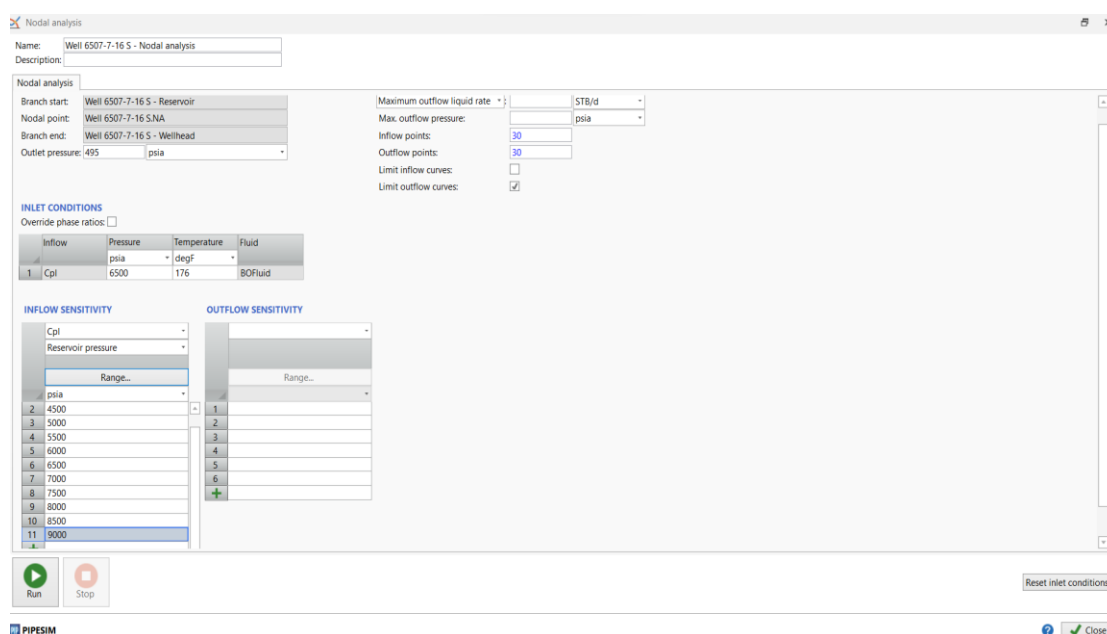


Figure 3.11: Nodal analysis properties

In order to run a nodal analysis simulation, the nodal analysis solution is selected in the main screen of PipeSim. Then, another screen appears, and pressure parameters are inserted for the first case of evaluating the tubing depth and size. Figure 3.11 presents the nodal analysis tab and required parameters for the analysis.

Figures 3.12 to 3.15 present the solution from the simulation in production (STB/d) as a function of the reservoir pressure boundary condition for different tube inner diameters ID = {2.375, 2.875, 3.5, 4.5} inch and different tubing embedment length $T_d = \{9636, 10123, 10450\}$ ft. Each group of bars refers to a different reservoir pressure boundary condition (P_r). We also considered a wellhead pressure P_{wh} (outlet pressure) equal with 495 psi. The explanation for this value is that the wellhead is located at some depth in the seabed. The seabed hydrostatic pressure value agrees with the 495 psi considered in the simulations. Finally, no data could be retrieved for this required variable, and this was the reasoning behind this value.

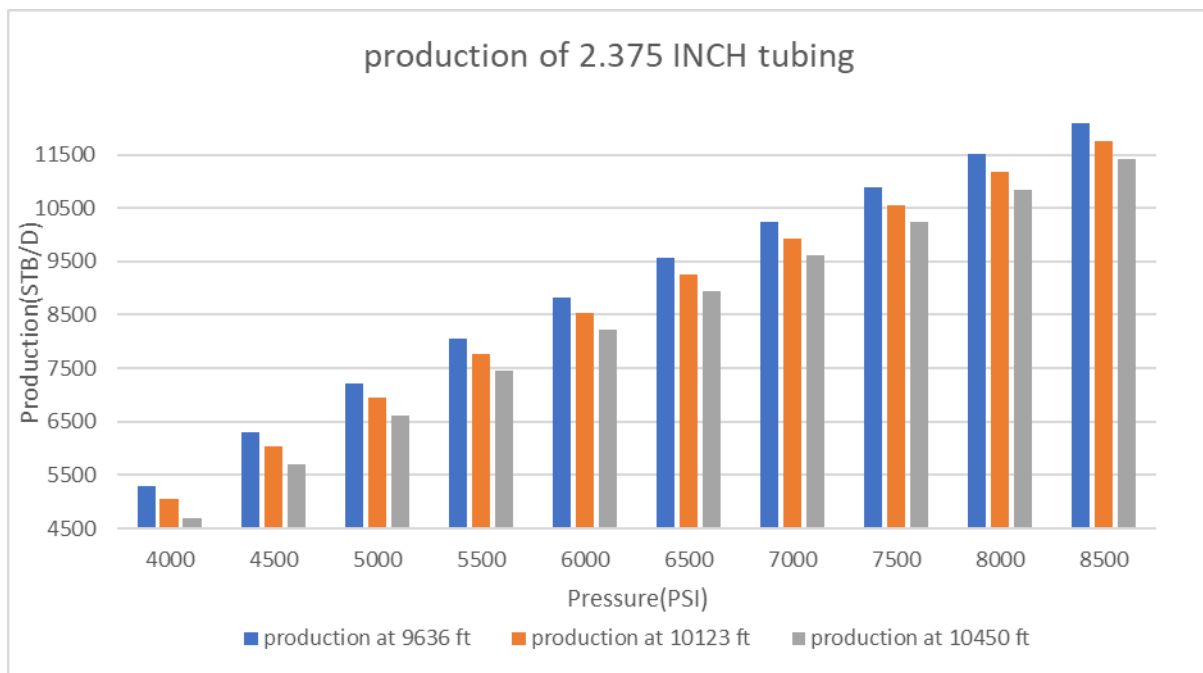


Figure 3.12 Production for tube size 2.375 and all tube embedment lengths

By examining Figure 3.12, it is seen, the best production rate is obtained when the tubing is placed at 9636 ft. As expected, with increasing the reservoir pressure boundary condition more production is obtained. In figure 3.13, the analysis with tube size 2.875 follows:

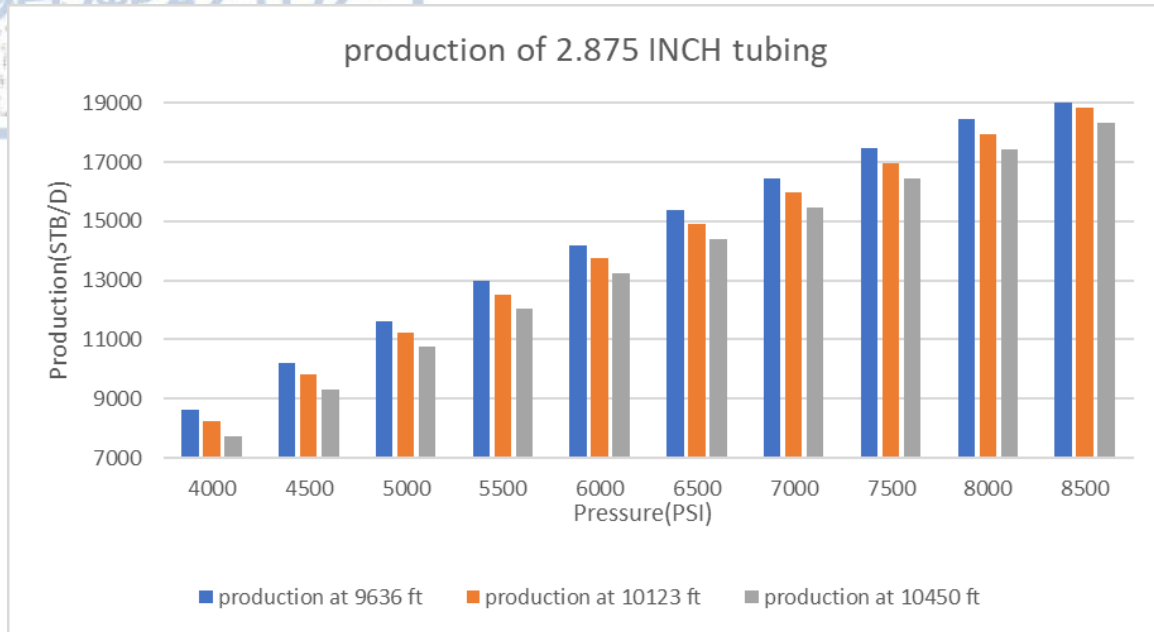


Figure 3.13 Production for tube size 2.875 and all tube embedment lengths

In this Figure 3.13, the production prediction follows the same trend. With increasing the tube size and the reservoir pressure boundary condition, more production is predicted by the simulator. Also, when the tube embedment length is shallower, then again, more production is predicted. In figure 3.14, the analysis with tube size 3.5 follows:

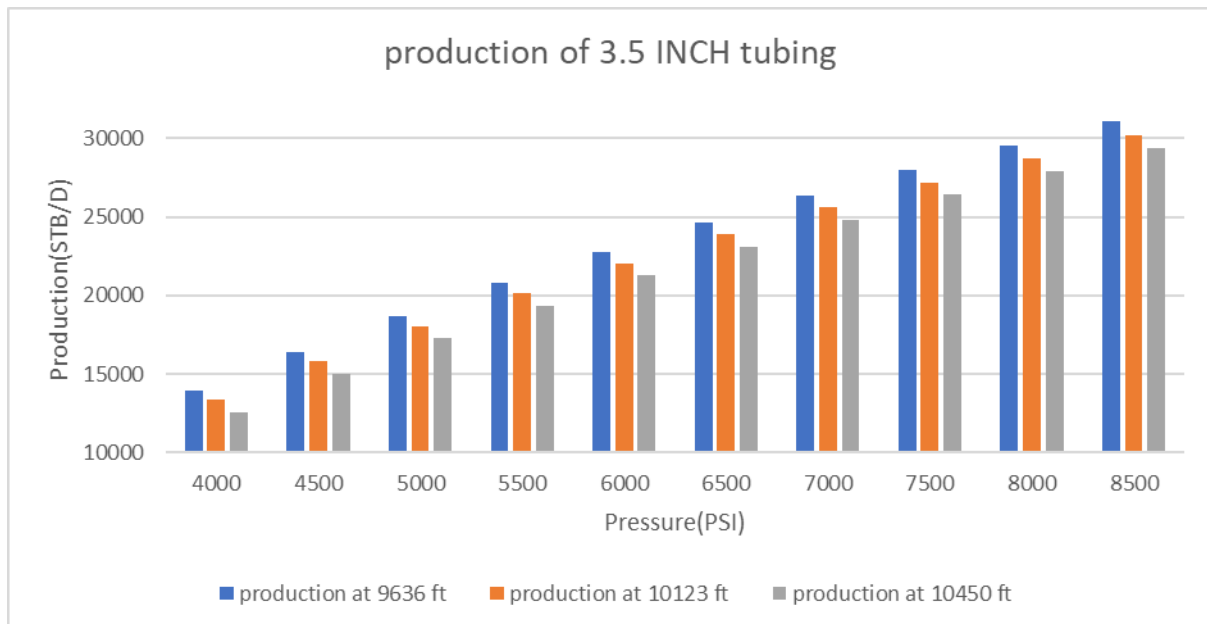


Figure 3.14 Production for tube size 3.5 and all tube embedment lengths

From Figure 3.14, the production prediction and in this simulation follows the same trend as the other two. By increasing the tube inner diameter and the reservoir pressure boundary condition, then greater production is obtained. As in the other two cases, when the tube embedment length is shallower, then greater production is favoured. In figure 3.15, the final analysis considered with tube size 4.5 follows:

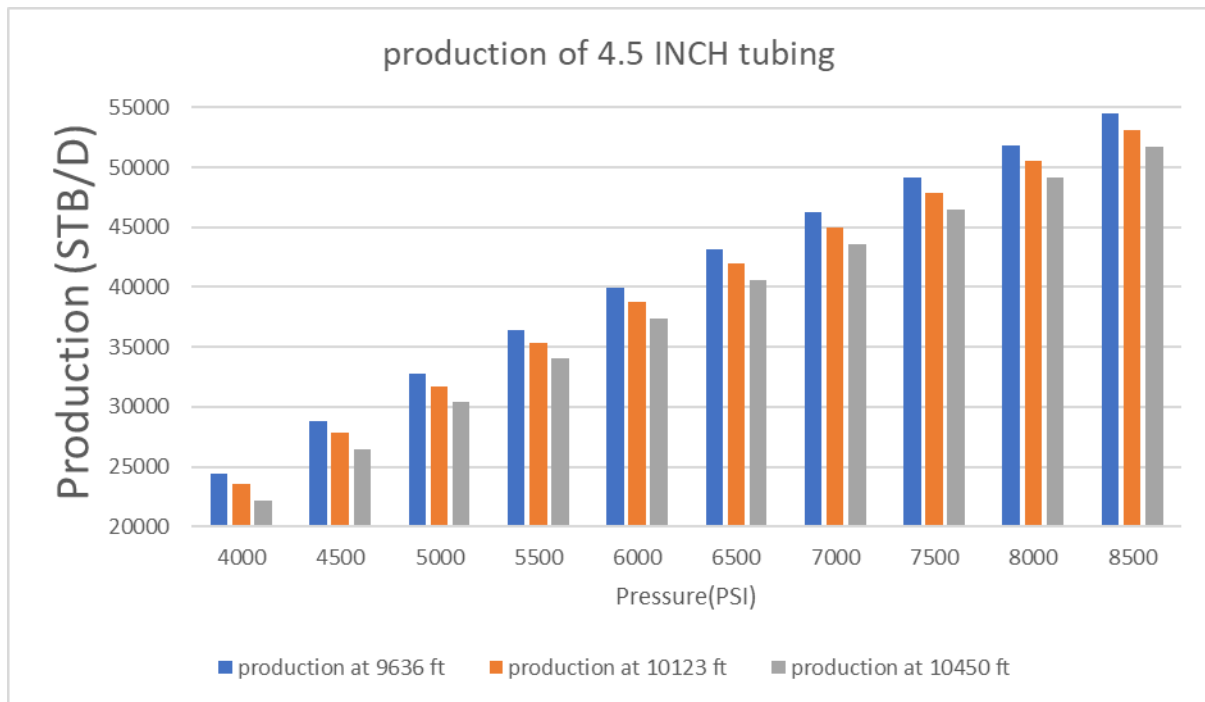


Figure 3.15 Production for tube size 4.5 and all tube embedment lengths

By examining Figure 3.15 same results are seen as the previous figures (3.12-3.14). Production prediction is a strong function of the reservoir pressure, tube inner diameter but also of the tube embedment. When compare between themselves with the degree of freedom being the tube inner diameter, as expected production is increased. A further, discussion involves the analysis of the data produced. We have analysed the production as a function of tube inner size diameter, and we have determined that production obeys a power law dependence as:

$$y = ax^n \Leftrightarrow y = ax^{2.35} \quad (3.1)$$

Where α is a coefficient (STB/day) and n is the power law index, to be fitted on the data and is about **~2.35** for all tube embedment lengths considered in the analysis.

Figure 3.16, presents the inflow and outflow performance graphs that are obtained after performing the nodal analysis with the well flow simulator. Each vertical line corresponds to a tube performance curve with different inner diameter tube size while the horizontal curves represent different inflow performance curves after declaring the pressure boundary conditions. (i.e. from 8500 psi to 4000 psi with 500 psi step). Their intersection point corresponds to the operating point of the well which is depicted with blue circle on the graph.

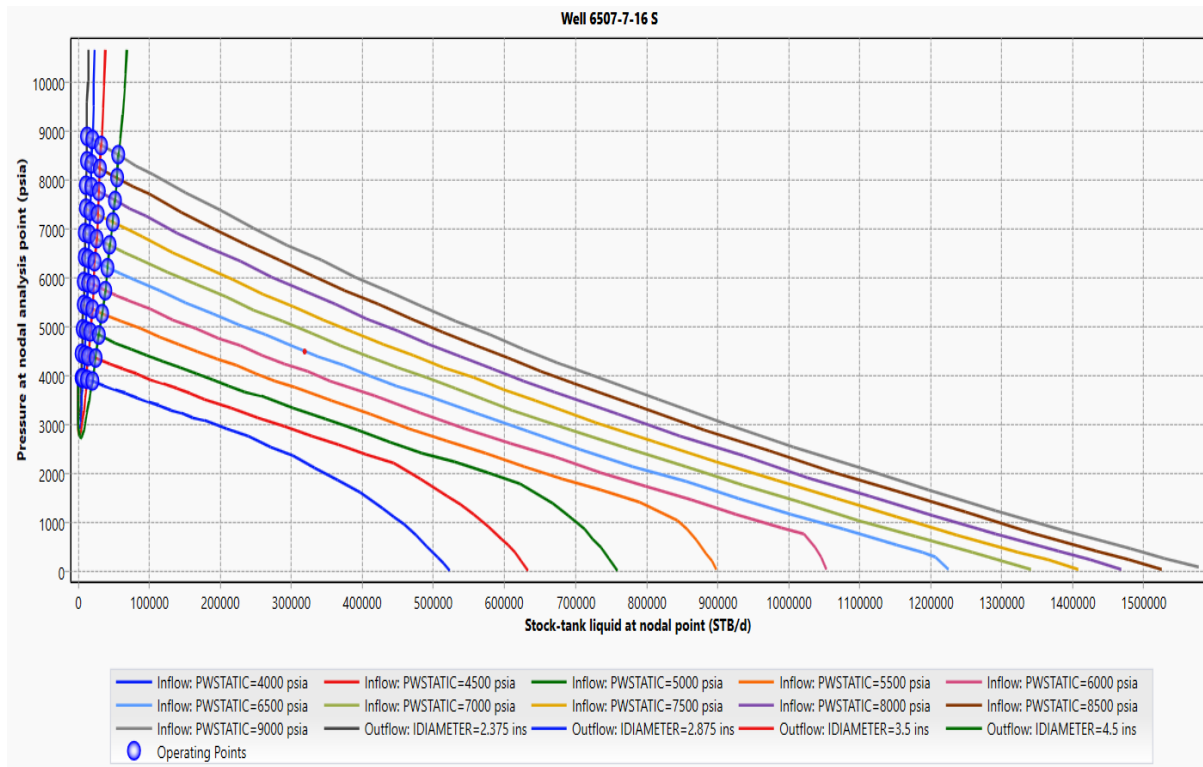


Figure 3.16 Inflow and outflow performance for all tube sizes considered

From this figure 3.16 we see that for high values of pressure boundary conditions, the inflow performance relationship remains linear but as the pressure boundary condition drops then it becomes non-linear. That is if linear up to a certain point and then begins to curve. This is explained by the fact that the pressure has dropped below the bubble point hence gases are expected during production making the inflow performance non-linear. From the point of view of time (corresponding to a simulation of reservoir pressure depletion 8500 psi to 4000 psi) each curve may represent a different snapshot in time. By examining the operating points, it is seen that production drops with pressure depletion. Also, this is true for all tube inner diameter selected for the purpose of this analysis. By data analysis, this confirms the previous finding regarding the power law dependence.

In general, the best-case scenario for the tube embedment length for all cases of pressure boundary conditions is the one with 9636 feet. Following this result, the rest of the analysis will be based on that case only. In addition, the best-chosen tubing is the one with the size of 4.5 inch. The scenario of the “*bigger the tubing, the more production*” indeed allows for higher production rates. However, this is not always the most desirable scenario in Oil and Gas companies, because the recoverable reserves may deplete faster than expected and the company will be forced to work for a short amount time. As such small tube prolongs the life of a well. Another important reason is the health and safety factor. According to Darcy, the bigger the pressure then the bigger the production thus increasing danger giving rise to phenomena like catastrophic failures and well leaks in the atmosphere.

At this point it should be noted that we only presented the results for the inflow and outflow performance for the tube embedment length 9636 for clarity reasons. The inflow and outflow performance figures were not reported because they present similar results.

In the following discussion we analyse the next bottom hole completion technique which is the open-hole a.k.a barefoot scenario. The procedure that was followed to construct the model in the simulator is the same with the only difference being on the “tabular tab” where we did not consider casing-cement and perforations. In the final casing option, the open hole is selected instead of the casing option and the rest of the procedure continues with the same way. In figure 3.17, the results from the simulations with an open-hole completion are presented.

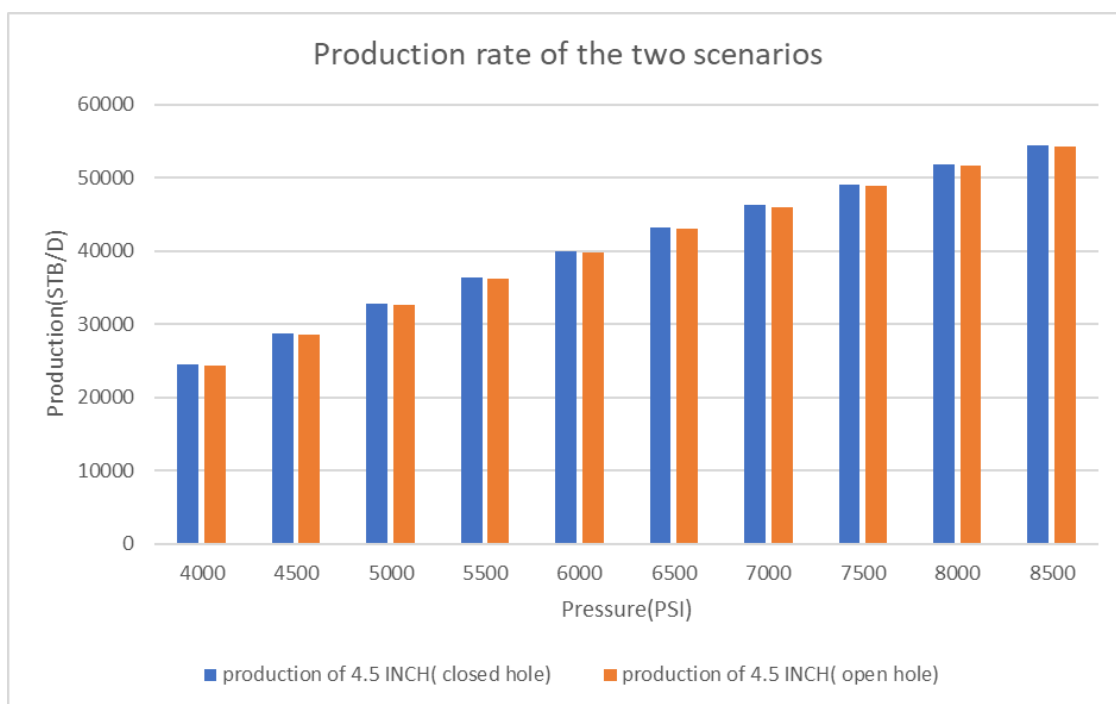


Figure 3.17 Comparison between open and closed hole

Figure 3.17 shows the solution for the two different bottom hole completion techniques in a comparison bar form. On the vertical axis we plot the production (STB/d) and in the horizontal axis we plot the reservoir boundary condition for the 4.5 tube inner diameter as promoted from the previous analysis and for the tube embedment length of 9.636 ft. We also considered a wellhead pressure P_{wh} (outlet pressure) equal with 495 psi.

As shown in Figure 3.17, the cased-cemented and perforated scenario has a better production rate. The advantage of a cased-hole completion is the ability to select zones to produce and a casing that supports the wellbore. However, perforations restrict the flow area and induce the flow to be concentrated in the near wellbore region, causing higher velocity than open hole scenarios. (Wan, 2011). Due to this concentrated flow and higher velocity the production rate appears to be better even in the same geological conditions. To summarize, the next part of the study will be conducted with the cased-cemented and perforated bottom hole completion technique adopting the tubing size 4.5 inch and the tube embedment length of 9.636 ft.

The next analysis is concerned with the sensitivity of the bean size of an SSSV. The main scope of the SSSV is to provide an emergency shutdown of the production when a high-risk situation occurs, for safety reasons. When active, they allow fluid flux but when closed no production is permitted. Table 3.2, presents in tabular form the production values for (i) different bean sizes and (ii) different installation depths.

Table 3.2: Production with different bean size and installation depth

		Production (STB/d)						
		Bean size (in)						
		1.875	2.125	2.313	2.562	2.813	3.75	3.813
Depth (ft)	350	12037.15	19238.47	19304.9	30714.94	30856	54175.77	54213.67
	750	12049.48	19269.2	19322.35	30774.06	30891.51	54232.28	54265.28
	1000	12053.54	19281.24	19330.21	30796.9	30904.85	54253.65	54282.79

As expected, the production rate is smaller with smaller SSSV bean size because with large bean size more fluid is allowed to pass through the SSSV. However, the installation depth appears to make no apparent difference. In other words, the depth of installation of the SSSV does not improve to any extent the simulated production. From this analysis, it is safe to conclude that installing a bigger SSSV and together with a bigger tubing size, the volume of hydrocarbon production will be higher than in situations where the equipment size will be smaller. Following this thought, the best depth to set the SSSV is at 1000 ft. This is also safer

for the equipment because its operational conditions will be lower temperature and pressure, so it may prolong its life expectancy before any serious equipment failure or maintenance of the well. Another important reason is the cost of maintenance. By installing pieces of equipment deeper in the well, the cost rises steeply and in cases where the equipment needs replacement or serviced, the deeper it is the more difficult and expensive it is to replace it.

3.2.3 The influence of water-cut on production

After some time of production, especially when the well is completed near or at some distance from the WOC, water makes its appearance in the production fluids. It has been observed that in extreme cases, water production can reach as high as 60% or even more. Of course, the presence of water creates operational difficulties during production because of the creation of emulsions changing dramatically the viscosity in the tube. As such, cost rises steeply and the operation becomes unprofitable (Watt, 2014; Ibrahim et al, 2021). A closer examination of the stratigraphy (Figure 2.2), well "31/3-3" is located above the water-oil contact (WOC). This means that the reservoir is higher than the WOC. On the other hand, there are no available data about the location of the WOC and placement of well "6507/7-16S" from the reports used to construct the models.

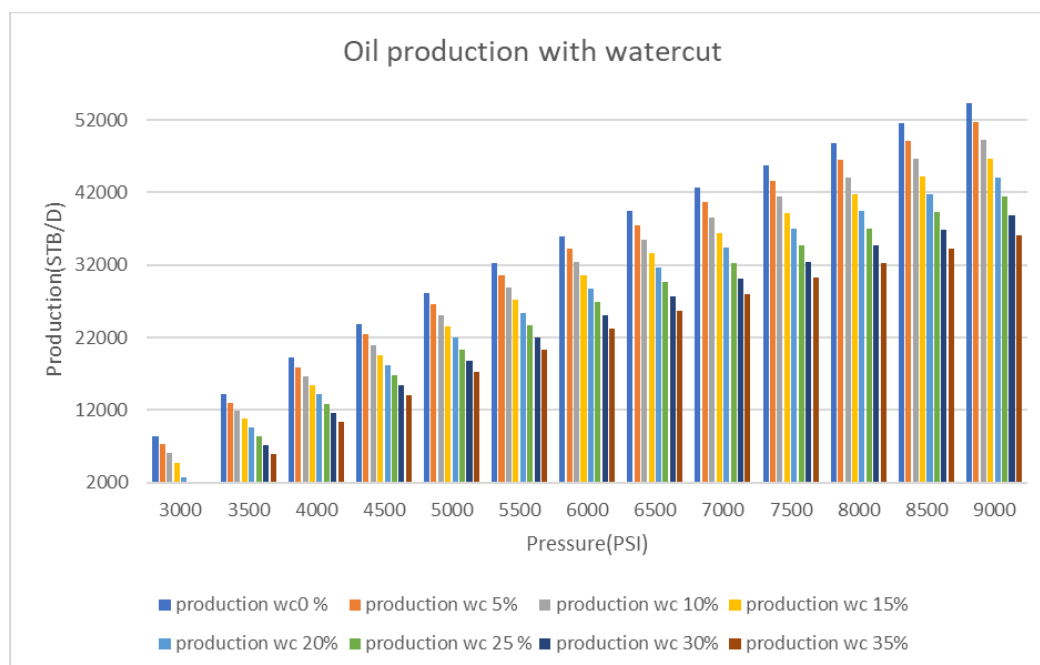


Figure 3.18: Oil production rate as a function of reservoir pressure for different values of water-cut {0:35:5}

So, in order to examine the influence of water presence in (%) in the simulated results of production, a series of models were run in PipeSim, ranging the water-cut in the data definition from {0-35} % with a step 5%. We choose these values for the simulations to have a physical meaning. Of course, higher values of water cut could be considered, however rendering the simulation physically inadmissible.

Figure 3.18 presents the oil production in STB/d as a function of reservoir pressure. Each group of bars represents different values of water-cut (e.g 0:35:5). By examining figure 3.18 we observe a linear decrease of oil production for all reservoir pressure conditions considered (3000-9000 psi). It is considered important to mention that the slope of each group of water-cuts changes with different values. Upon further analysis, we observe that the linearity that exists in the reduction of production for the oil under simultaneous production of water is about ~ 0.053 , with negative sign dictating slow reduction. On the other hand, if higher values of water-cut would be considered, then the linearity in physics might change to non-linear.

During production, gas is expected to be produced. Especially, when GOR = 628 SCF/bbl is considered in the simulations. It is therefore of paramount importance to also investigate the production Gas in the simulations as a function of the water production. Figure 3.19 presents the gas production in mmscf/d as a function of reservoir pressure. Each group of bars represents the different values of water-cut considered in the previous simulations (0:35:5).

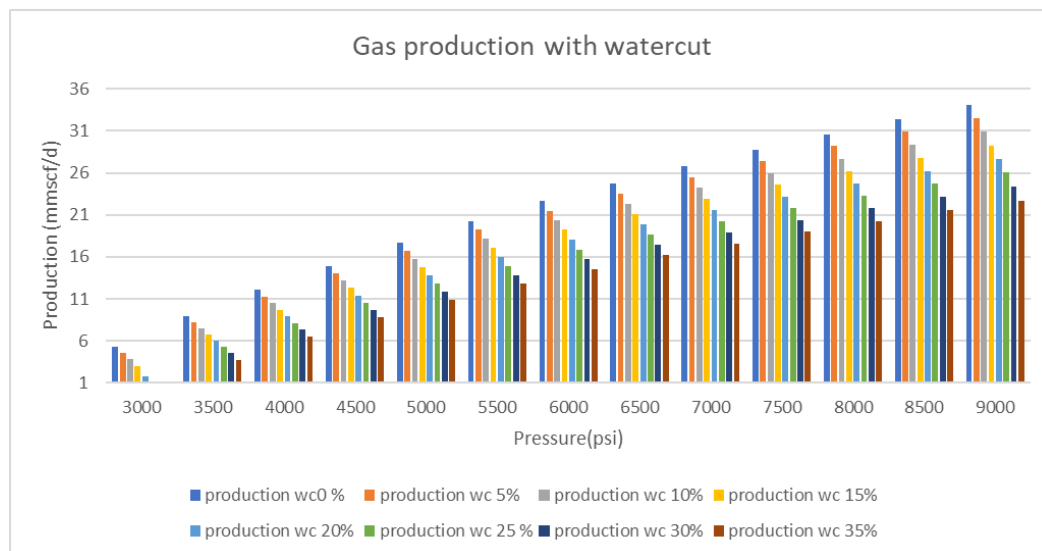


Figure 3.19: Gas production after inserting watercut

A closer look of figure 3.19 we observe again a linear decrease of gas production for all reservoir pressure conditions considered (3000-9000 psi). However, the magnitude of gas

production is significantly lower as compared to oil production. Also, in the case of gas production the slope of each group of water-cuts changes with different numbers. Performing data analysis, we observe that the reduction of gas production under simultaneous production of water is about $\sim 3.326 \times 10^{-5}$, with negative sign dictating that the production of gas does not dominate the production system (i.e. does not influence significantly the oil production with any of the water cuts considered) and hence the linear reduction. In cases where the gas production would dominate, one would expect that the production and reduction would be influenced according to Darcy's law (dp^2/dr).

3.2.4 The influence of skin factor of well "6507/7-16S"

Skin factor is a numerical value that quantifies the formation damage. That is, it quantifies any changes in the permeability causing abstraction to fluid flow. In analytical terms it is an important parameter in the Darcy differential equation which affects the pressure drop (a.k.a drawdown pressure) considered to be the driving force of transmissibility of fluids. Problems with formation damage is usually encountered in wells that are active for a certain period. A good application of numerical simulations with PipeSim is the evaluation of well performance under the influence/action of skin. For the purposes of this analysis, we have considered 3 different values of skin {1, 3 and 5} for all reservoir pressure conditions considered combined with water cut 35%.

Figures 3.20 and 3.21 present the oil and gas production as a function of the reservoir pressure conditions considered respectively, for zero water cut (WC=0%) while figures 3.22 and 3.23 present the same graphs for the worst-case scenario (WC=35%). All figures 3.20 to 3.23 are plotted for skin factor values $S=1, 3, 5$ (-). The analysis of these figures gives the opportunity to investigate 2 degrees of freedom. (i) The influence of the skin factor but also (ii) the influence of the water-cut on the simulated results of Oil and Gas production. This analysis serves also as material balance of the produced fluids.

As it can be seen when examining the influence of the skin for each reservoir pressure boundary condition, little influence is observed in the oil and gas production attributed to the skin for both water-cut values considered (0 & 35%). On the other hand, when examining the oil and gas production for the different water-cuts, a serious reduction in both oil and gas production is observed owing to the presence of water. Specifically, for the highest reservoir pressure boundary condition (9000 psi) a reduction of the order of **14k STB/d** is observed for the oil production while **11 mmSCF/d** is observed for the gas production.

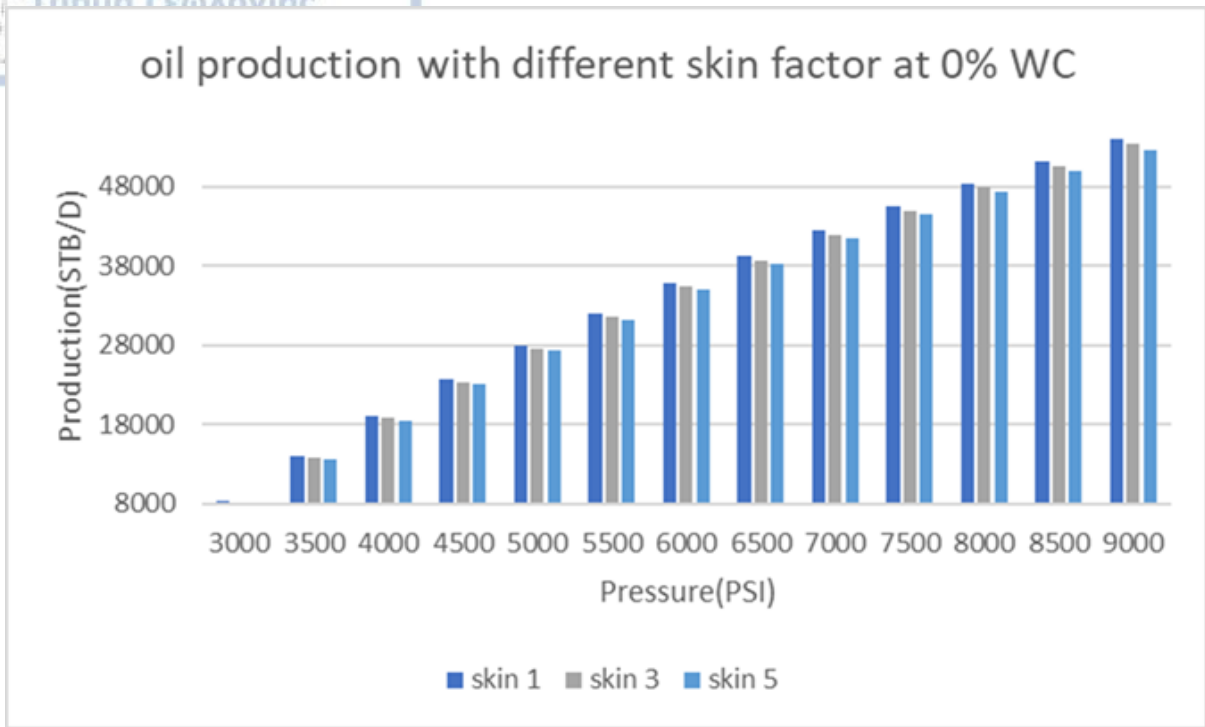


Figure 3.20: Oil production with different skin factors for 0% water-cut

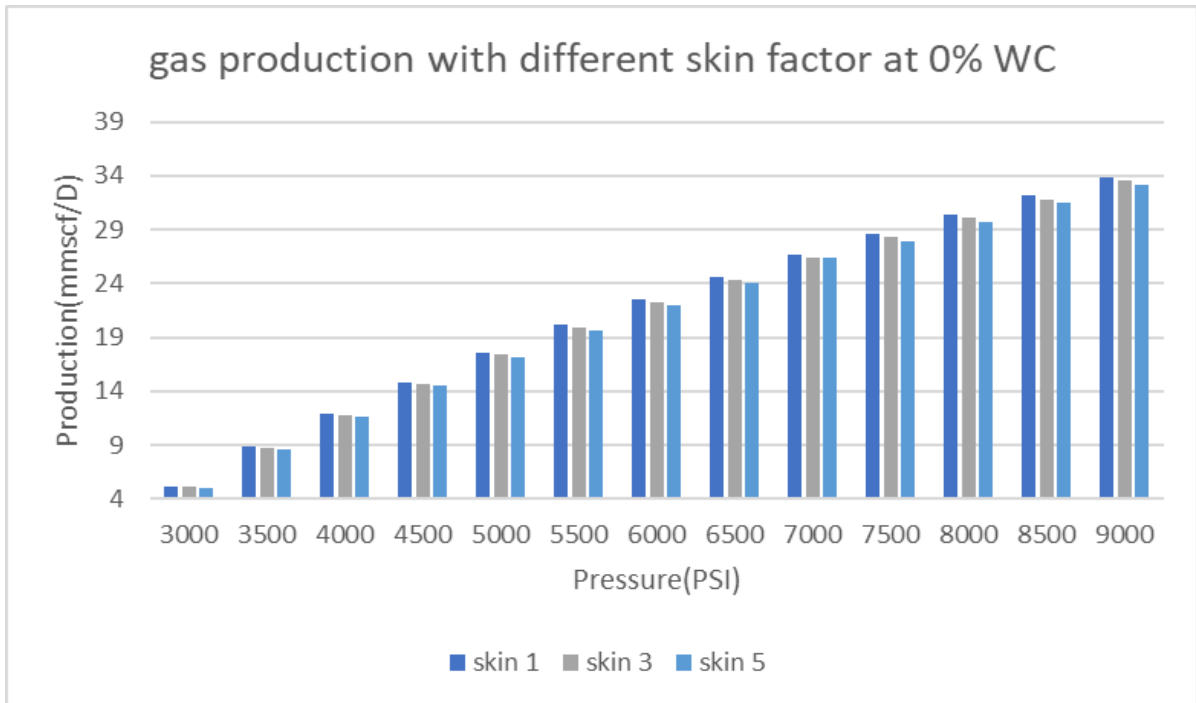


Figure 3.21: Gas production with different skin factors for 0% water-cut

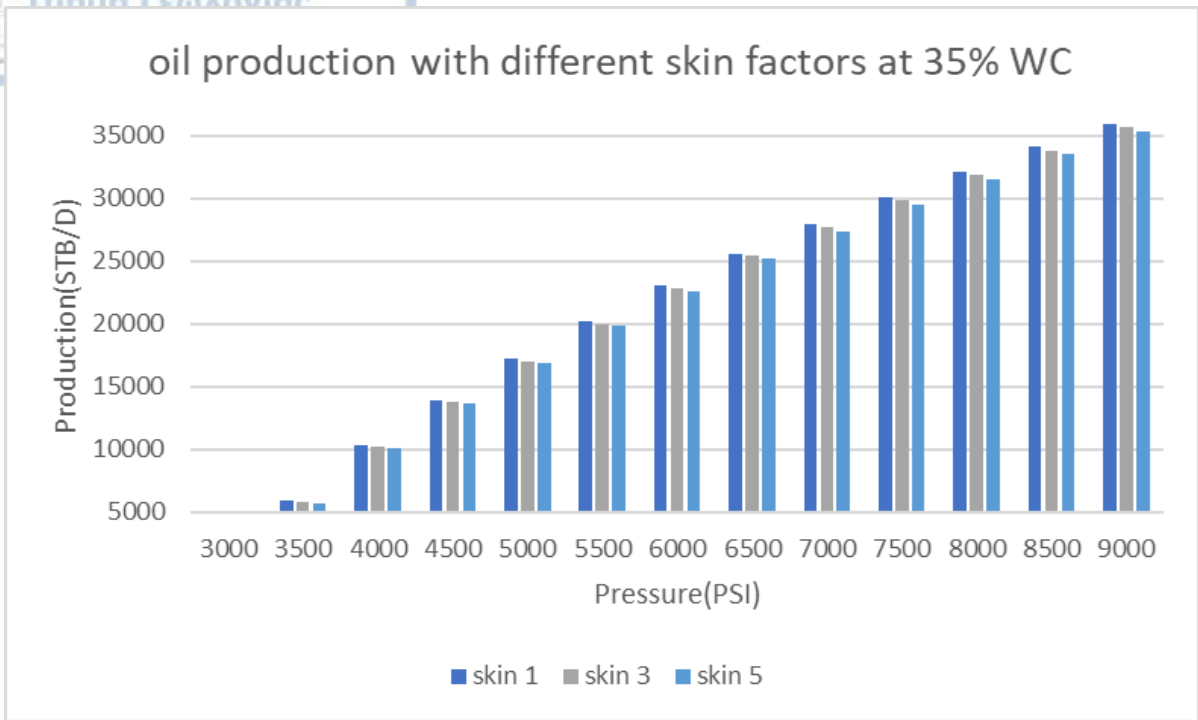


Figure 3.22: Oil production with different skin factors for 35% water-cut

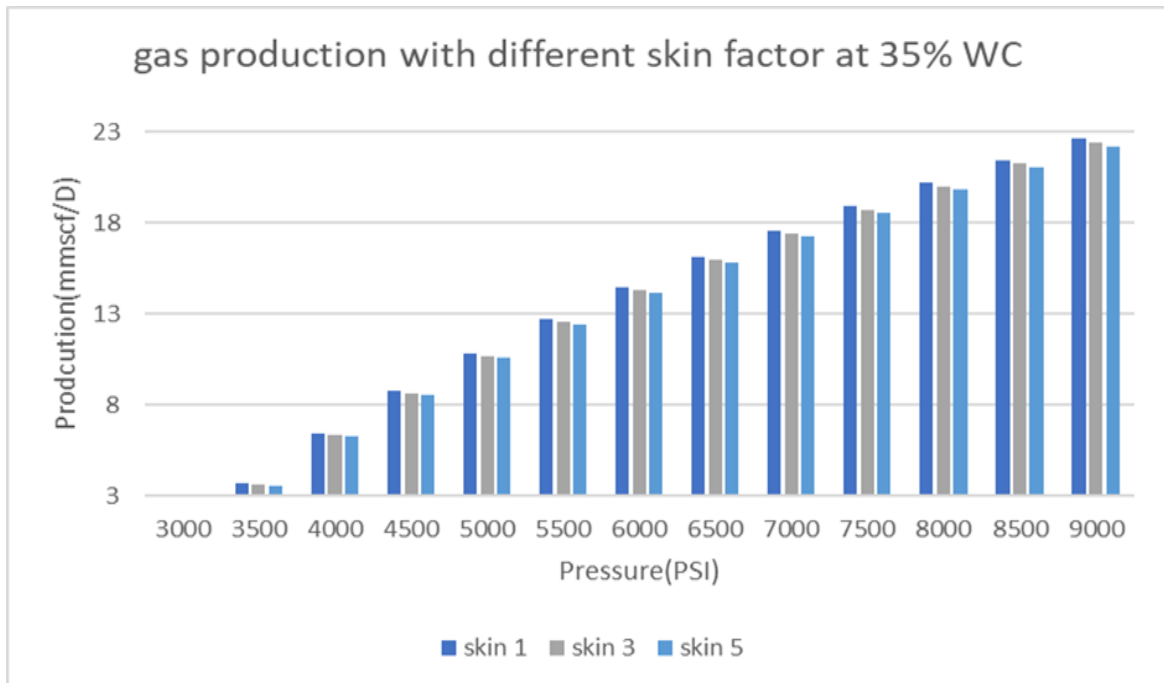


Figure 3.23: Gas production with different skin factors for 35% water-cut

3.2.5 Construction and production simulation of well “well 31/3-3”

For the construction of “well 31/3-3” the same techniques were adopted as the previous well. The equipment and completion design that were promoted from the well “6507/7-16S” simulation was examined as the best-case scenario and no further sensitivity or parametric investigation was considered. So, the same equipment and similar depths were used, in order to examine the overall completion efficiency on a different well, but with similar rock and fluid characteristics. Figure 3.24 presents the general tab for the new well “well 31/3-3”.

General	Tubulars	Deviation survey	Downhole equipment	Artificial lift	Heat transfer	Completions	Surface equipment
Well name: 31/3-3(reference)							
Active: <input checked="" type="checkbox"/>							
Well type: <input checked="" type="radio"/> Production <input type="radio"/> Injection							
Check valve setting: Block reverse							

Figure 3.24: General data of the “well 31/3-3”

Next, we define the locations of the casings, tubing, and other necessary definitions for the simulation from the tubulars tab as shown in Figure 3.25. By comparing figures 3.25 and 3.4 the main differences can be seen between the two simulated wells.

General	Tubulars	Deviation survey	Downhole equipment	Artificial lift	Heat transfer	Completions	Surface equipment
Mode: <input type="radio"/> Simple <input checked="" type="radio"/> Detailed							
Dimension option: <input type="radio"/> OD <input checked="" type="radio"/> Wall thickness							
CASINGS/LINERS							
Section type	Name	From MD	To MD	ID	Wall thickness	Roughness	
		ft	ft	in	in	in	
1	Casing	1279,528	2857,612	30	0,361	0,001	...
2	Casing	1279,528	3920,604	20	0,2983471	0,001	...
3	Casing	1279,528	6581,365	13,375	0,2241526	0,001	...
4	Casing	1279,528	9721,129	9,135305	0,1530992	0,001	...
TUBINGS							
Name	To MD	ID	Wall thickness	Roughness			
	ft	in	in	in			
1	Tubing	6582,526	4,5	0,4567652	0,001	...	

Figure 3.25: Well construction (geometry) and material data for the "well 31/3-3"

The differences are mainly at the setting depths of the equipment and the geometrical diameters. In comparison with the well “6507/7-16S” this well “31/3-3” is shallower. There are also three casings only, instead of four presented in well “6507/7-16S”. The final bottom hole completion technique is the same, cased-cemented and perforated. The first three casings of the two wells match in the inner diameter (ID) counting from the lower well. The difference

is the borehole final TVD and penetration length. Namely, well “6507/7-16S” has TVD = 10,623 ft and tube embedment length = 9,636 ft while well “31/3-3” has TVD = 9,721 ft inches and tube embedment length = 6,500 ft. For the rock, we have considered the same porosity, and average reservoir permeability. The reservoir pressure boundary condition was considered nearly the same as the previous simulations, ranging from 2000 psi to 9000 psi with 500 psi step.

The next part of the analysis is the evaluation of the completion string design equipment. As mentioned earlier, it remains the same as the well “6507/7-16S”, with the only difference being the setting depth. Figure 3.26 presents the completion equipment considered for the well “31/3-3”.

General					Tubulars					Deviation survey					Downhole equipment					Art				
		Equipment		Name		Active		MD																
								ft																
1	SSSV		SSSV			<input checked="" type="checkbox"/>		2279,528																
2	Sliding sle...		Sleeve			<input type="checkbox"/>		3679,528																
3	Packer		Pk			<input checked="" type="checkbox"/>		6082,526																
4			NA			<input checked="" type="checkbox"/>		7103,018																
+																								

Figure 3.26: Downhole equipment used for the simulation of well “31/3-3”

The packers were placed 500 ft above the pay-zone, as it was done in the reference well “6507/7-16S”, but due to the fact that this well is much shorter, the setting depth was set to 6082 ft. The SSSV and SSD were placed 2279 ft and 3679 ft respectively for the same reasons mentioned in the reference well “6507/7-16S”. To summarize, the final model that was created in PipeSim is presented in Figure 3.27 All the equipment and the settling depths are presented in this model. It is also noticeable that the final penetrated horizon is much longer than the one in the reference well. The perforations were placed by the same logic, a little bit deeper than the tubing and with the same parameters as in the well “6507/7-16S”.

The fluid model that was used has the same reservoir and oil characteristics as the previous model. The reasoning for this is that the two wells are in the same area (North and Norwegian Sea). Table 3.3 presents the fluid model definition that was used in this simulation. The input data are inserted in the completions tab.

Table 3.3 Rock and Fluid properties definitions for well "31/3-3"

Parameter	Values
Reservoir thickness, d (ft)	498
Average porosity, Φ (%)	29
Range of field permeability, k (md)	670-19500
Average used in simulations, k (md)	1450
Oil column, h (m)	195
Average reservoir pressure, P_r (psi)	2600
Average reservoir temperature, T_r ($^{\circ}$ F)	100
Well diameter, r_w (inch)	12.25
Drainage radius, r_e (ft)	2000

Summarizing, the average reservoir pressure is much smaller in this well than the reference well.

3.2.6 Simulation results for the well "31/3-3"

The results from the simulations are presented in figure 3.30. It is important to note that for pressure boundary conditions lower than 3000 psi, the oil production becomes very small. Also, by considering the fact that the reservoir has pressure of about 2600 psi, the decision for plug and abandon was a proper one. In a different scenario, where the pressure could have been 9000 psi, the production was going to be of economic importance, however, such elevated pressure is not realistic for this kind of reservoir. Also, it is very important to note that current Enhanced Oil Recovery (EOR) methods are too expensive to increase the reservoir pressure from the biggening of the wells' life. As such, the production cost deemed the well as "unprofitable" for the company. For educational purposes though, a big range of pressure was tested in order to be comparable with the reference well. Figure 3.28, presents the numerical simulation for the production in bbl/d for the different ranges of pressure boundary conditions.

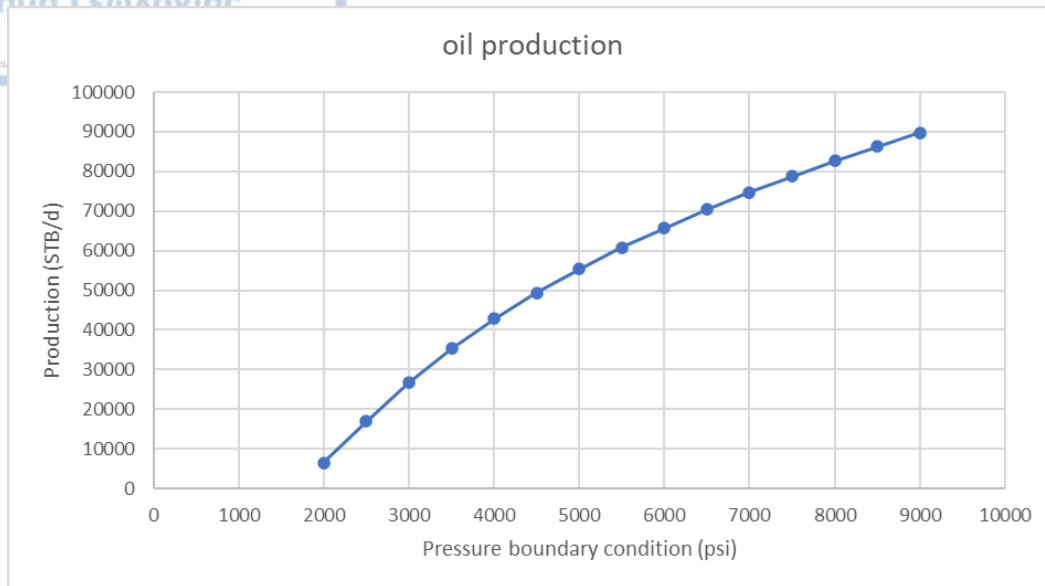


Figure 3.28: Oil production for different reservoir pressure for the well "31/3-3"

As shown in figure 3.28, the production in quite improved with the fictitious pressure boundary conditions above 2600 psi. This result is also related with the tubing size diameter which is 4.5 in and the reservoir properties (sandstone). Also, the considered reservoir has excellent permeability of about 1000 md after hydraulic fracturing. However, there aren't any available data for skin, so the influence of the skin will be investigated parametrically in the following sections. The following figure 3.29 presents the comparison for the production between the two wells.

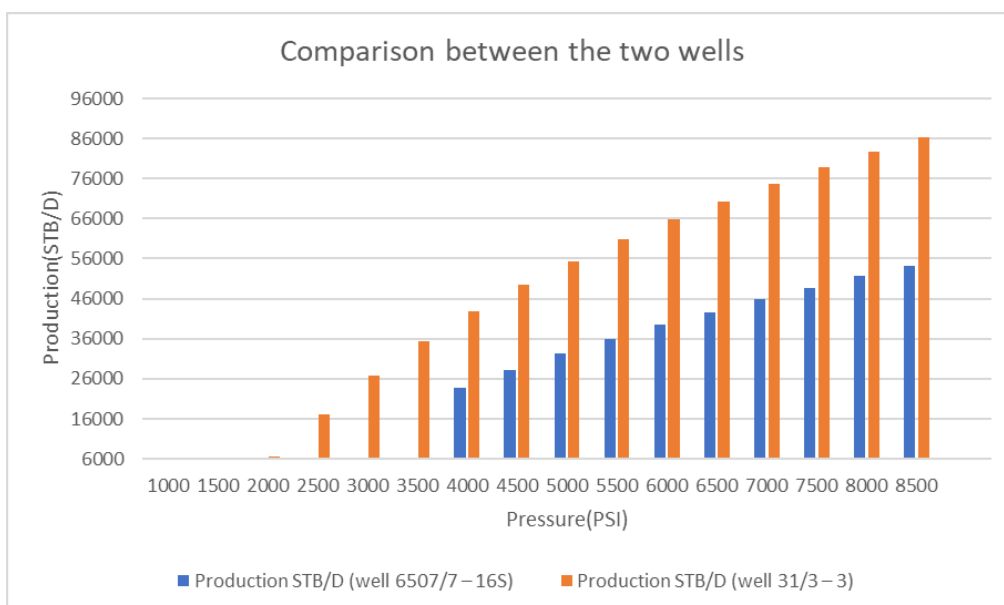


Figure 3.29: Oil production comparison between the two wells

As explained earlier, the well “6507/7-16S” was simulated within the pressure range of 4000-8500 psi while the well “31/3-3” was simulated within the pressure range of 2000-8500 psi. For this reason, comparison data for the first pressure levels {2000-3500 psi} there aren’t any available for comparisons for well “6507/7-16S”. By examining figure 3.29, it is evident that the well “31/3-3” has a better production rate considering the fact that both simulated wells have the same equipment in any of the corresponding pressure boundary conditions. The higher production rate of well “31/3-3” can be explained by its shorter length as compared to well “6507/7-16S”.

Figure 3.30, shows the inflow and outflow performance graphs that were obtained with the nodal analysis method. The vertical line corresponds to the tube performance (ID: 4.5 in) while the horizontal curves represent different inflow performance curves corresponding to different pressure boundary conditions ranging from 2000 to 8500 psi allowing a 500 psi step. Their intersection point corresponds to the operating point shown with blue circle on the graph.

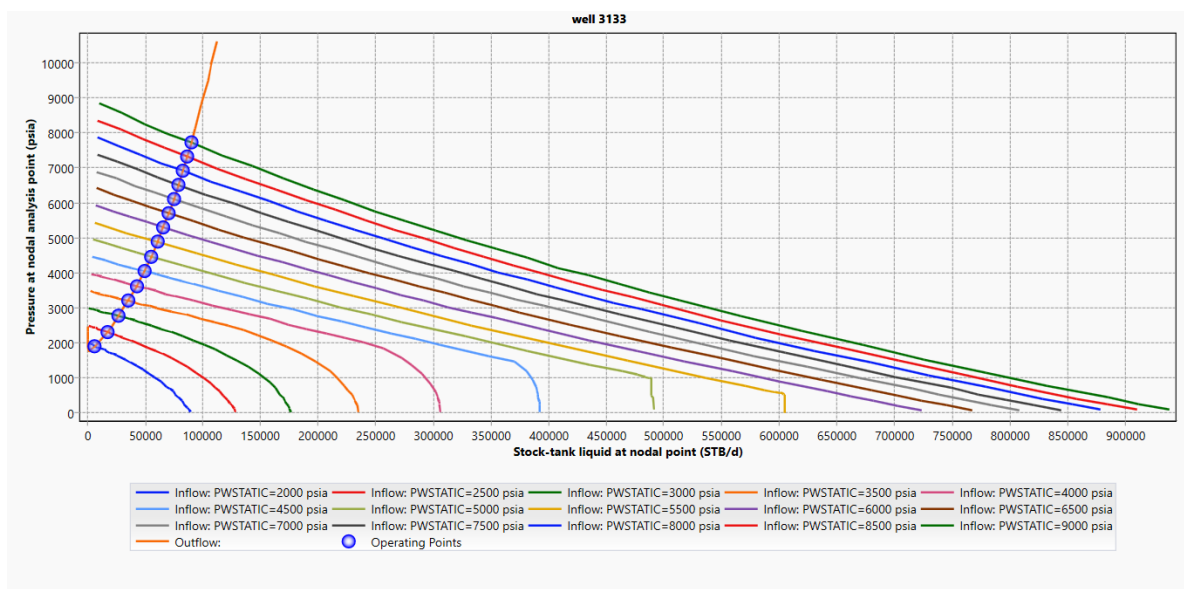


Figure 3.30 Inflow and outflow performance for all reservoir boundary pressure conditions

From figure 3.30 we see that for high values of pressure boundary conditions, the inflow performance relationship remains linear but as the pressure boundary condition drops then it becomes non-linear most probably because pressure has dropped below the bubble making the inflow performance non-linear. From the point of view of time (corresponding to a simulation of reservoir pressure depletion 9000 psi to 2000 psi) each curve may represent a different snapshot in time. By examining the operating points, it is seen that production drops with pressure depletion.

3.2.7 The influence of skin factor of well “31/3-3”

The analysis in this section is concerned with the influence of the skin factor for well “31/3-3”. As in the previous analysis we could have investigated the influence of the water-cut on the produced results, but as already mentioned, this well is located quite higher from the WOC zone thus we did not consider it in the simulations. In other words, the following results are for WC=0%.

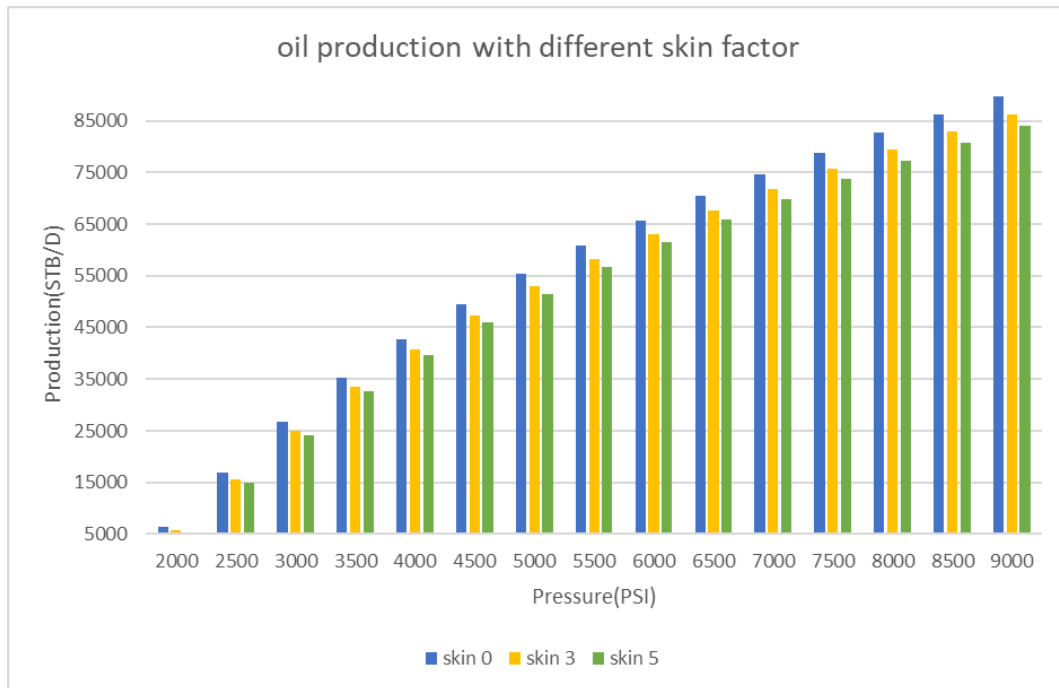


Figure 3.31: Oil production rate after inserting skin factor

Figure 3.31 presents the oil production as a function of reservoir pressure conditions. Each group of bars corresponds to a different reservoir pressure condition and each bar is for a different value of skin as shown in the figure 3.31 legend. By examining the behavior depicted in figure 3.31, as expected, the higher the value of the skin, the lower the production. Notably, for the case of very low reservoir pressure condition and high value of skin factor production is minimized to the point of nearly zero production (order of few hundred STB/d). For further data analysis we plot Figure 3.32 which shows the production reduction owing to skin effects. Equation (3.2) presents the calculation of the reduction in the production as percentage.

$$\text{Production reduction (\%)} = \frac{(Ideal_{s=0} - Ideal_{s=5})}{Ideal_{s=0}} \times 100 \quad (3.2)$$

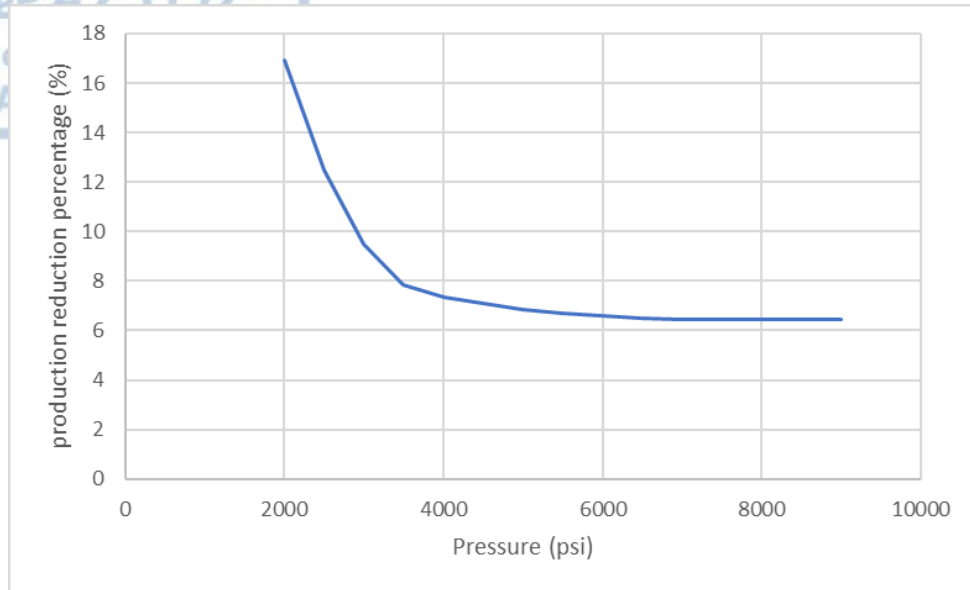


Figure 3.32: Percent reduction in oil production due to skin

The physical interpretation of figure 3.32 is that for lower reservoir boundary condition, the reduction in oil production could be as high as **16%** but with increasing the reservoir pressure boundary condition and after the certain threshold of 6000 psi (depending on the input data used for the simulations), the oil production reduction tends to a constant value of about **6.5%**. This means that with whatever pressure conditions prevail in the reservoir (e.g higher than 6000 psi) a constant reduction attributed to the skin will be present. Such results are highly useful for making decisions as to when the well should undergo workovers and maintenance.

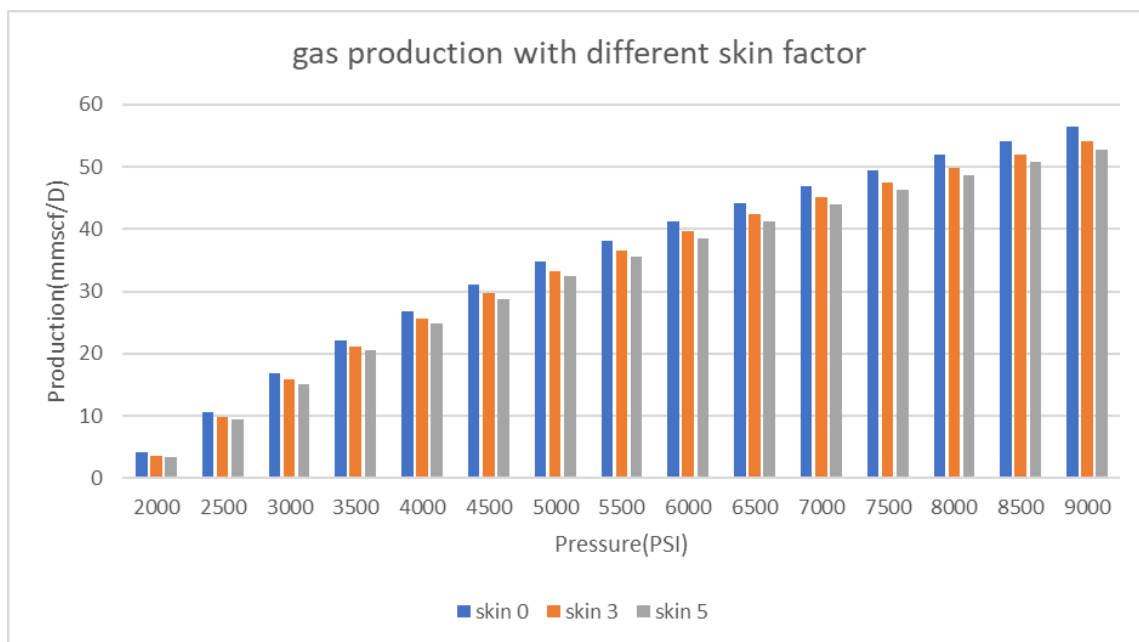


Figure 3.33: Gas production rate after inserting skin factor

As already mentioned, due to the well input parameters, production of gas is expected during the operation of the well. Figure 3.33 presents the gas production as a function of reservoir pressure conditions. Each group of bars represents the 3 different values of skin considered in the simulations $\{S= 0, 3, 5\}$. Results are presented for WC=0%. From figure 3.33, as expected, the higher the value of the skin, the lower the production. Also, the skin affects significantly the production of gas in low reservoir boundary conditions as analysed in the oil production.

3.3 Comparison of results

The final part of this chapter is a discussion for the two wells that were simulated. It should be mentioned that this work is based on a set of assumptions due to the usual lack of data that companies do not provide without confidentiality agreements and to the authors knowledge we have performed the simulations as close as it can reach to actual conditions. Also, no second well is the same as another despite the fact that they are constructed in a similar geological environment and conditions presenting similar characteristics, they will eventually have a different production.

3.3.1 Comment on the outflow performance

Although the geological conditions are very similar to both wells, some differences exist. First, the TVD is different with also different embedment depths. Also, the geology affects all five elements of conventional petroleum in sandstones (i) petroleum generation, (ii) migration, (iii) trap, (iv) reservoir, (v) cap/seal rock, which eventually play a major role in the production rate simulations. To have comparable results we have considered the same pressure boundary conditions ranging from 2000 to 9000 psi while simulating both wells but also keeping the same input data (reservoir, rock and fluids and completion string facilities). As such, the only degree of freedom affecting production is the well configuration through the length of the well. It is known that the physical variables resisting flow are (i) the pressure of the wellhead (P_{wh}) and (ii) the hydrostatic pressure which is $P_{hyd} = \rho gh$. In combination they sum $P_{wh} + \rho gh$ to resist flow. Equation (3.3) shows the conditions for production from a well:

$$\begin{aligned} \bar{P}_r > P_{wh} + P_{hyd} &\Leftrightarrow Lift \\ \bar{P}_r \leq P_{wh} + P_{hyd} &\Leftrightarrow No Lift \end{aligned} \quad (3.3)$$

where \bar{p}_r is the average reservoir pressure, p_{wh} is the wellhead pressure and p_{hyd} is the hydrostatic pressure. Equation (3.4) presents the influence of well length in production.

$$\begin{aligned}\bar{p}_r > p_{wh} + \rho_m g (h_{well1} = 10623 \text{ ft}) &\Leftrightarrow \text{Low Production} \\ \bar{p}_r > p_{wh} + \rho_m g (h_{well2} = 7103 \text{ ft}) &\Leftrightarrow \text{High Production}\end{aligned}\quad (3.4)$$

where ρ_m is the density of the mixture (i.e oil, gas and water), g is the acceleration of gravity and h_{well} is the two wells length measured from the wellhead to the perforations (where fluid enters the well: communication point). From the above analysis, more production is expected from the shorter well.

3.3.2 Comment on inflow performance

Although both wells have similar characteristics, there are some differences between them, that makes them produce and work differently. As mentioned, in order to have a more accurate comparison and data evaluation, the second well, had to be similar to the first one, that's why a well from the same region was chosen to optimize its production, and it was located near the first having also similar (not same) depths and penetrated horizons.

Continuing the discussion from section 3.3.1 it is important to mention that the final completion depth also plays a major role in the production by affecting the average reservoir pressure (see eq 3.3 & 3.4). Let us examine the case of the shallow well ($h=7103$ ft). By keeping the hydraulics of the completion, the same as the deep well ($h=10623$ ft) and comparing them for the same reservoir pressure condition each time, the inflow performance is expected to be higher in the shallow well case. One may argue that when compared with same reservoir pressure might be an erroneous comparison because reservoir pressure is a function of depth and density (unit weight) of overlaying rocks according to:

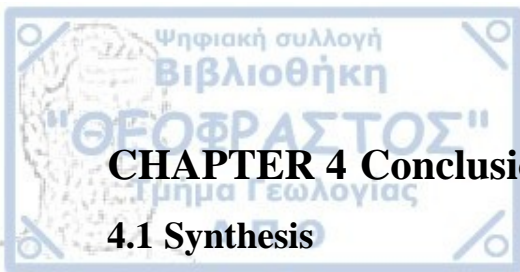
$$\begin{aligned}\sigma_v &= \sum_{i=1}^n \gamma_i h_i \quad (\text{Vertical stress creation}) \\ \sigma_h &= k \sigma_v \quad (\text{Horizontal stress creation})\end{aligned}\quad (3.5)$$

where, σ_v is the vertical stress applied on the reservoir rock, γ_i is the unit weight of each layer from the surface to the depth of the cap/seal rock, h_i is the thickness of each rock from the surface to the depth of the cap/seal, n is the number of rocks, k is the lateral earth thrust

coefficient which is strong function of the Poisson ratio ν and σ_h is the horizontal stress. Then these two boundary conditions (both vertical and horizontal) are translated inside the reservoir according to Terzaghi's and Biot's theory (effective stress principles) as:

$$\begin{aligned}\sigma_{Total}^{Terzaghi} &= \sigma_{Effective}^{Terzaghi} + P \quad (Terzaghi) \\ \sigma_{Total}^{Biot} &= \sigma_{Effective}^{Biot} + aP \quad (Biot)\end{aligned}\tag{3.6}$$

where σ is the total stress in both theories has the same definition (stress transferred on the solid skeleton of the rock and the fluid(s) inside the reservoir rock), σ' is the effective stress (what is carried by the solid skeleton only of the reservoir rock), P is the pressure term of the fluids that also undertake part of the stresses caused by equations (3.6), and a is the biot coefficient (or poroelastic constant) that takes into account the compressibility of the fluids inside the reservoir. Biot coefficient takes theoretical values between (0-1). When the value is zero then it means we have absence of fluid (dry rock) and when the value is unity then it means that we have fully incompressible fluids. A closer look of equation (3.6), the Terzaghi definition is the special case of Biot's definition for incompressible fluids. In real reservoirs, Biot coefficient takes values between 0.25-0.5 with usual being 0.35 (Economides and Nolte, 2000). Considering the above analysis, the difference in depth (3520 feet), plays a major role in the pressure creation in the reservoir which influence production and overall well performance.



CHAPTER 4 Conclusions

4.1 Synthesis

The purpose of this work was to study the completion of the well “6507/7-16S” and well “31/3-3” in Norway. For the purpose of this work, we have performed a detailed literature review for the two wells regarding the geology and technical characteristics in order to find the depths of the casings, to check the installation depths of the completion string equipment, such as packers, safety valves, sliding sleeves and type of tubing. These we used as input data for the well simulator PipeSim, by next-Schlumberger. As soon as the models were constructed a set of simulations were conducted to investigate the parameters that influence the inflow and outflow performance of the constructed wells and where we had absence of input data we performed detailed sensitivity analysis. The simulations were conducted in the spirit of the numerical method of Nodal analysis and the produced results were critically evaluated.

4.2 Findings

The summarized results of this research work are the following:

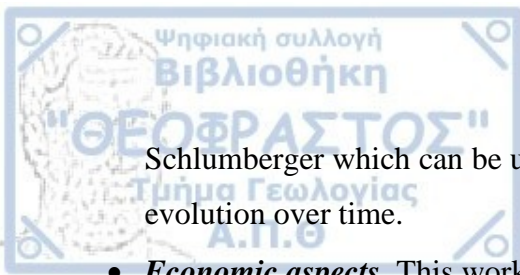
- The two wells with very similar characteristics, with the same equipment, but at different completion depths, produced different outflow performance. Appropriate modifications were made to keep the two wells’ characteristics as close as possible to enable comparisons and understand the physics affecting outflow performance. From this analysis we have seen that again the bottom-hole completion technique and the well embedment in the reservoir plays a major role in the overall well performance.
- Water simultaneously produced with hydrocarbons is shown to be important in affecting outflow performance and hence the pure hydrocarbon production rate. From the input data considered, water can enter the well reducing oil and gas production.
- Simultaneous gas production (GOR=628 SCF/STB) from the simulations appeared to have little effect in outflow performance. In general, it affects the overall density (makes the produced fluid lighter) thereby assisting flow without creating slug effects. This is also a strong function of the input data used in the simulations.
- The skin factor appeared to have little effect at high reservoir pressure boundary conditions. For the set of input data used, production becomes insensitive to the skin (i.e produces the same volume of hydrocarbons) when the reservoir pressure boundary condition is higher than 5000 psi. On the other hand, it costs to the overall well performance 6% reduction, for both wells simulated.

- The considered pressure of the reservoir is one of the most important factors because it regulates inflow and outflow performance and hence hydrocarbon production. The pressure range for the first well was considered to be 4000 - 9000 psi, with a 500 psi step, produced significant amount of hydrocarbons. For the second well, the pressure range considered was somewhat lower 2000-9000 psi again with a step of 500 psi, because the well was completed in a shallower depth. From the analysis performed, we have shown that both completed wells can produce significant volumes of hydrocarbons even for relatively low reservoir pressures. This is however a strong function of the permeability that was considered (which was assumed to be quite high but representative of a hydraulically fractured stimulated reservoir). It is reminded that the range of reservoir pressure conditions considered covers the full range of reservoirs pressure, from low to highly pressurized rock formations as hypothetical scenarios.
- Finally, oil production appears to follow a power law dependence (with power law index = ~ 2.35) with inner tube diameter for all range of reservoir pressure boundary conditions considered in the simulations.

4.3 Suggestions for improvement

The results presented in this research work present merely a first approach to the problem. This work could be improved with further study of the completions string facilities to simulate as best as possible inflow and outflow issues. Below, we outline few suggestions for further improvements:

- **Reduce the working assumptions.** As stated, the simulations with the well simulator Pipesim will be significantly improve with actual input data thereby reducing the working assumptions of this work.
- **Establish a perforation strategy.** Well simulator PipeSim provides the capability to study different configurations of perforations, such as multiples, sub-angles, different phases, stand-off from well e.t.c. In this work all the above have not been studied.
- **Transient analysis.** The analysis reported in this work reflects a more steady-state simulation of well performance. This means that the pressure-drop as a function of production with time cannot be captured. To capture this behavior, we studied different snapshots in time by assuming a start reservoir pressure and with a step of 500 psi reduction to drop to a minimum. This assumption, could be overcome by using OLGA, by next-

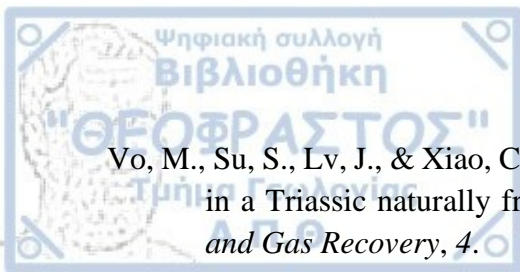


Schlumberger which can be used for simulating the transient part of the problem involving evolution over time.

- **Economic aspects.** This work was focused on the completions and hydraulics aspect of the problem. We have not performed any financial analysis with respect to the cost of completion string facilities-equipment which is very important in decision making or requesting for further coupled engineering-economic analysis for optimizing both completions and costs.

References

- Ahmed, H., Mallah, S. A., Anwar, M. T., Ali, M., Ali, S. D., Javed, W. A., & Usman, M. (2023). Understanding Your Wells: Conventional Nodal Analysis; Not a Solution for Depleting Fields. SPE Gas & Oil Technology Showcase and Conference. SPE.
- Anovitz, L. M., & Cole, D. R. (2015). Characterization and analysis of porosity and pore structures. *Reviews in Mineralogy and geochemistry*, 80(1), 61-164.
- Bellarby, J. (2009). *Well completion design*. Elsevier.
- Brown, K. E. (1982). Overview of artificial lift systems. *Journal of Petroleum Technology*, 34(10), 2384-2396.
- Brown, K. E., & Lea, J. F. (1985). Nodal systems analysis of oil and gas wells. *Journal of petroleum technology*, 37(10), 1751-1763.
- Copestake, P., Sims, A. P., Crittenden, S., Hamar, G. P., Ineson, J. R., Rose, P. T., ... & Bathurst, P. (2003). The Millennium Atlas: Petroleum geology of the central and northern North Sea.
- Dimo, P. (1975). *Nodal analysis of power systems*. Editura Academiei Republicii Socialiste România.
- Economides, M. J., & Nolte, K. G. (2000). *Reservoir stimulation*. 3rd Edition, Wiley.
- Eiken, O., & Tøndel, R. (2005). Sensitivity of time-lapse seismic data to pore pressure changes: Is quantification possible? *The Leading Edge*, 24(12), 1250-1254.
- Filgueiras, P. R., Sad, C. M., Loureiro, A. R., Santos, M. F., Castro, E. V., Dias, J. C., & Poppi, R. J. (2014). Determination of API gravity, kinematic viscosity and water content in petroleum by ATR-FTIR spectroscopy and multivariate calibration. *Fuels*, 116, 123-130.
- Georgakopoulos (2020), *Petroleum Geology lectures*. Hydrocarbons exploration and exploitation MSc programme.
- Hovland, M. (1983). Elongated depressions associated with pockmarks in the western slope of the Norwegian Trench. *Marine Geology*, 51(1-2), 35-46.
- Ibrahim, A. F., Al-Dhaif, R., Elkhatny, S., & Shehri, D. A. (2021). Applications of Artificial Intelligence to Predict Oil Rate for High Gas–Oil Ratio and Water-Cut Wells. *ACS omega*, 6(30), 19484-19493.
- Johnson, H., Leslie, A. B., Wilson, C. K., Andrews, I., & Cooper, R. M. (2005). *Middle Jurassic, Upper Jurassic and Lower Cretaceous of the UK Central and Northern North Sea*. British Geological Survey.
- PipeSim (2017) "User's manual", Next-SLB
Saga Petroleum, Final well report 31/3-1
- Sarris (2019). *Fluid flow in porous media lectures*. Hydrocarbons exploration and exploitation MSc programme.
- Smith, K., Gatliff, R. W., Smith, N. J. P., & Hillis, R. R. (1994). Discussion on the amount of Tertiary erosion in the UK estimated using sonic velocity analysis. *Journal of the Geological Society-London*, 151(6), 1041.
- Theuerkorn, K. (2012). Reservoir characterisation using macromolecular petroleum compounds including asphaltenes: A case study of the Heidrun oil field in the Norwegian North Sea.



Vo, M., Su, S., Lv, J., & Xiao, C. (2020). Reservoir modeling and production history matching in a Triassic naturally fractured carbonate reservoir in Sichuan, China. *Improved Oil and Gas Recovery*, 4.

Wan, R. (2011). *Advanced well completion engineering*. Gulf professional publishing.

Watt, H. (2014). *Production Technology*. Institute of petroleum engineering, Heriot Watt University.

Zolotukhin, A. B. (1979, April). Analytical definition of the overall heat transfer coefficient. In SPE California Regional Meeting. OnePetro.

Internet resources

- [https:// www.camtop-oilfieldtools.com/](https://www.camtop-oilfieldtools.com/)
- [https:// www.factpages.npd.no/](https://www.factpages.npd.no/)
- [https:// www.gbpipe.com/](https://www.gbpipe.com/)
- [https:// www.iadclexicon.org/](https://www.iadclexicon.org/)
- [https:// www.oilandgasoverview.com/](https://www.oilandgasoverview.com/)
- [https:// www.production-technology.org/](https://www.production-technology.org/)
- [https:// www.ruifengpetrotech-en.com/](https://www.ruifengpetrotech-en.com/)
- [https:// www.superiorenergy.com/](https://www.superiorenergy.com/)
- <https://www.drillingmanual.com/>
- <https://www.epa.gov/ui/>
- <https://www.halliburton.com/>
- <https://www.petroleum.co.uk/>
- <https://www.slb.com/en/>